Comparative study of the Grüneisen parameter for 28 pure fluids

Peter Mausbach,[1] Andreas Köster,[2] Gábor Rutkai,[2] Monika Thol,[3] and Jadran Vrabec[2, a)]

[1)] *Cologne University of Applied Sciences, 50678 Köln/Germany*

[2)] *Thermodynamics and energy technology, Universität Paderborn, 33098 Paderborn/Germany*

[3)] *Thermodynamics, Ruhr-Universität Bochum, 44801 Bochum/Germany*

(Dated: 1 July 2016)

The Grüneisen parameter γ_{G} is widely used for studying thermal properties of solids at high pressure and also has received increasing interest in different applications of non-ideal fluid dynamics. Because there is a lack of systematic studies of the Grüneisen parameter in the entire fluid region, this study aims to fill this gap. Grüneisen parameter data from molecular modelling and simulation are reported for 28 pure fluids and are compared with results calculated from fundamental equations of state that are based on extensive experimental data sets. We show that the Grüneisen parameter follows a general density-temperature trend and characterize the fluid systems by specifying a span of minimum and maximum values of γ_{G}. Exceptions to this trend can be found for water.

Keywords: Grüneisen parameter; liquid state thermodynamics; fundamental equation of state; molecular simulation.

[a)] Corresponding author. E-mail address: jadran.vrabec@upb.de

I. INTRODUCTION

The dimensionless Grüneisen parameter γ_{G} is generally used as a thermomechanic property characterizing solids at high pressure.In terms of the lattice vibration spectrum of solids, individual mode Grüneisen parameters are defined by[1]

$$\gamma_{\mathrm{i}} = -\frac{v}{\omega_{\mathrm{i}}} \left(\frac{\partial\, \omega_{\mathrm{i}}}{\partial\, v} \right)_T , \tag{1}$$

where ω_{i} is the frequency of each mode, v is the volume and T the temperature. A macroscopic Grüneisen parameter can be derived as an average of the γ_{i} leading to[1]

$$\gamma_{\mathrm{G}} = v \left(\frac{\partial p}{\partial e} \right)_v = \frac{v}{c_v} \left(\frac{\partial p}{\partial T} \right)_v = \frac{\rho}{T} \left(\frac{\partial T}{\partial \rho} \right)_s , \tag{2}$$

in which p is the pressure, e the internal energy, c_v the isochoric heat capacity, ρ the density and s the entropy. For solids, γ_{G} is often assumed to be independent of the temperature T. Incorporating further thermodynamic response functions into Eq. (2) allows for the derivation of additional identities for the Grüneisen parameter

$$\gamma_{\mathrm{G}} = \frac{v\, \alpha_p}{c_v\, \beta_T} = \frac{v\, \gamma_v}{c_v} = \frac{\alpha_p\, w^2}{c_p} , \tag{3}$$

with the isobaric heat capacity c_p, the thermal expansion coefficient $\alpha_p = \frac{1}{v} \left(\frac{\partial v}{\partial T} \right)_p$, the isothermal compressibility $\beta_T = -\frac{1}{v} \left(\frac{\partial v}{\partial p} \right)_T$, the thermal pressure coefficient $\gamma_v = \left(\frac{\partial p}{\partial T} \right)_v$ and the speed of sound w. In addition to its relevance in the solid state, the Grüneisen parameter has received increasing interest in fluid states because γ_{G} ubiquitously appears in different applications of non-ideal fluid dynamics.

Arp et al.[2] published a significant study of this parameter for hydrodynamic processes of compressible fluids. They discussed the Grüneisen parameter in the context of Fanno,

Rayleigh and isentropic flows and listed a number of variants of equations used for both mass and energy conservation in which γ_{G} can be expressed. An important outcome of their work is the nature of this parameter near the critical point, where it appears to vanish similar to the speed of sound.

A criterion required for the existence of shock waves in compressible fluid dynamics can be formulated by using the fundamental derivative of gas dynamics[3]

$$\Gamma = 1 + \frac{\rho}{w}\left(\frac{\partial w}{\partial \rho}\right)_s, \tag{4}$$

where the sign of Γ determines the existence and stability of shock waves. $\Gamma > 0$ is required for classical compressive shock waves. However, some exeptional fluids may have the property of a negative Γ and are called *Bethe-Zel'dovich-Thompson* (*BZT*) fluids. They exhibit a nonclassical gas dynamic behavior in the single-phase vapor region, through the existence of rarefaction shock waves[4]. Menikoff and Plohr[5] showed how properties of shock waves and rarefaction waves are determined solely by the adiabatic exponent $\kappa = -\frac{v}{p}\left(\frac{\partial p}{\partial v}\right)_s$, the fundamental derivative Γ and γ_{G}, which illustrates the importance of the Grüneisen parameter for this interesting situation.

The Grüneisen parameter was also found to be relevant in density scaling concepts of supercooled liquids[6]. A key quantity in this approach is the density scaling exponent γ that controls relaxation times, depending on density and temperature as a function of ρ^{γ}/T. It is of great interest to derive the density scaling exponent γ in terms of the Grüneisen parameter γ_{G}. In a recent study[7], the interrelation between γ_{G} and γ, as used in the analysis of so-called *Roskilde* - simple liquids[8], was studied in detail for a Lennard-Jones system in a larger fluid region.

Furthermore, the Grüneisen parameter is found to be a prominent quantity when ana-

lyzing geophysical problems in the Earth's core[9,10]. Finally, because the Grüneisen parameter establishes a link between thermal and caloric properties, it has become increasingly important for the development of fundamental equations of state (EOS), verifying their qualitatively correct thermodynamic behavior[11,12].

Despite the fact that the Grüneisen parameter γ_G exhibits a key role in such diverse fields of fluid dynamics, it is surprising that systematic studies of this quantity in the entire fluid region are limited or are quite old[13–18]. Therefore, it is desirable to evaluate this parameter for various atomic and molecular systems for a large region of the fluid phase. It is the aim of this study to investigate the Grüneisen parameter by using a direct molecular simulation method and to compare these theoretical results with those obtained from aggregated experimental data.

This paper is organised as follows. First, a brief overview of the employed molecular simulation method is given. Next, the Grüneisen parameter is analyzed for 28 pure fluids by comparison of the simulation results with EOS recommended by the National Institute of Standards and Technology (NIST). As a measure to characterize the differences between the various fluids, the range of minimum and maximum values of the Grüneisen parameter γ_G are given in a tabulated form. Finally, a conclusion is drawn.

II. MOLECULAR SIMULATION METHOD

On the basis of a molecular interaction model for a given substance, molecular simulation allows, in principle, for the investigation of any thermodynamic property without any restrictive approximation. The statistical mechanical formalism proposed by Lustig[19,20] constitutes the theoretical framework of the present work and was designed to provide an arbitrary number of Helmholtz energy derivatives from a single molecular simulation run for

a given state point. The reduced Helmholtz energy

$$\frac{A}{RT} \equiv \alpha(\tau,\delta) = \alpha^{\mathrm{o}}(\tau,\delta) + \alpha^{\mathrm{r}}(\tau,\delta)\ , \tag{5}$$

is commonly divided into an ideal (superscript "o") and a residual (superscript "r") contribution in which R is the molar gas constant, $\tau = T_{\mathrm{c}}/T$ is the inverse reduced temperature and $\delta = \rho/\rho_{\mathrm{c}}$ the reduced density, where T_{c} is the critical temperature and ρ_{c} the critical density. The ideal contribution $\alpha^{\mathrm{o}}(\tau,\delta)$ corresponds to the value of $\alpha(\tau,\delta)$ when no intermolecular interactions are at work. The formalism proposed by Lustig was implemented into the molecular simulation tool *ms*2[21,22] that yields up to eight derivatives of the residual Helmholtz energy

$$A^{\mathrm{r}}_{mn} = \tau^m \delta^n \frac{\partial^{\,m+n}\alpha^{\mathrm{r}}(\tau,\delta)}{\partial\,\tau^m \partial\,\delta^n} = (1/T)^m \rho^n \frac{\partial^{\,m+n}\alpha^{\mathrm{r}}(T,\rho)}{\partial(1/T)^m \partial\rho^n}\ . \tag{6}$$

With this method, the analytical derivatives of Eq. (6) can directly be sampled in order to investigate the Grüneisen parameter. In terms of Helmholtz energy derivatives the isochoric heat capacity can be expressed by $c_v = -R\,(A^{\mathrm{o}}_{20} + A^{\mathrm{r}}_{20})$ and the pressure derivative with respect to the temperature by[23] $(\partial p/\partial T)_v = R\,\rho\,(\,1 + A^{\mathrm{r}}_{01} - A^{\mathrm{r}}_{11})$. Inserting it in the second expression of Eq. (2) gives

$$\gamma_{\mathrm{G}} = -\,\frac{1 + A^{\mathrm{r}}_{01} - A^{\mathrm{r}}_{11}}{A^{\mathrm{o}}_{20} + A^{\mathrm{r}}_{20}}\ . \tag{7}$$

Note that an ideal gas contribution $A^{\mathrm{o}}_{20} = 1 - c^{\mathrm{o}}_p/R$ is present in the denominator, where c^{o}_p is the isobaric heat capacity of the ideal gas. In this study we apply c^{o}_p models corresponding to the most recent and most accurate fundamental equations of state.

For the 28 pure fluids analyzed in this study each system was sufficiently equilibrated for 10^5 cycles at each state point, and then sampled for $1 \cdot 10^6$ to $2 \cdot 10^6$ production cycles

in canonic (NVT) ensemble Monte Carlo simulations (number of particles N, volume V and temperature T were held constant). The number of particles was set to $N = 256$ to 864. Note, that no significant system size effects were encountered. The electrostatic long-range corrections were considered by the reaction field method[24]. Rigid and non-polarizable molecular interaction models were taken from the literature as summarized in Table 1. All of these models consist of one or more Lennard-Jones 12-6 potential interaction sites in order to describe the dispersive and repulsive interactions. For the polar interactions a varying number of point charges, point dipoles or point quadrupoles was employed. Detailed descriptions of the models are given in the original publications listed in Table 1. The statistical uncertainties of the simulation data were estimated by block averaging and the error propagation law.

III. RESULTS AND DISCUSSION

The Grüneisen parameter for different fluid systems obtained from present simulations was compared with those obtained from accurate EOS. These EOS were carefully correlated to the entire experimental data base. Details of the ansatz procedures may be found in the references summarized in Table 1. For this study, these EOS were evaluated by the program RefProp 9.1[25] distributed by the NIST. To facilitate the comparison of the results, critical point coordinates ($T_\mathrm{c}, p_\mathrm{c}, \rho_\mathrm{c}$), the triple point temperature T_tr and the molar weight M are listed in Table 1. For most substances, the temperature dependence of the Grüneisen parameter γ_G along isochores is discussed. In the following figures, symbols represent molecular simulation results and the solid curves the corresponding EOS. Dashed curves represent extrapolations of the EOS. The Grüneisen parameter along the vapor-liquid coexistence line is shown as a dotted line. The statistical uncertainties of the simulation data are typically

TABLE I. Critical data (T_c, p_c, ρ_c), triple point temperature T_{tr}, molar weight M as well as references for equations of state (EOS) and molecular interaction models (IM) applied for the 28 pure fluids. Thermodynamic data are from experiments.

Substance	T_c[K]	p_c[MPa]	ρ_c[mol/l]	T_{tr}[K]	M[g/mol]	EOS	IM
Acetone	508.1	4.7	4.7	178.5	58.079	[27]	[50]
Ammonia	405.4	11.33	13.21	195.5	17.03	[28]	[51]
Argon	150.69	4.863	13.407	83.806	39.948	[29]	[52]
Benzene	562.02	4.907	3.901	278.67	78.112	[30]	[53]
Carbon Dioxide	304.13	7.377	10.625	216.59	44.01	[31]	[54]
Carbon Monoxide	132.86	3.494	10.85	68.16	28.01	[27]	[55]
Chlorobenzene	632.35	4.521	3.24	227.9	112.557	[32]	[53]
Cyclohexane	553.6	4.081	3.224	279.47	84.159	[33]	[56]
Dimethylether	400.38	5.337	5.94	131.66	46.068	[34]	[57]
Ethane	305.32	4.872	6.857	90.368	30.069	[35]	[52]
Ethanol	514.71	6.268	5.93	159.0	46.068	[36]	[58]
Ethylene	282.35	5.042	7.637	103.99	28.054	[37]	[52]
Ethylene Oxide	468.92	3.705	7.17	160.65	44.053	[38]	[59]
Fluorine	144.41	5.172	15.603	53.481	37.997	[39]	[52]
Hexamethyldisiloxane	518.75	1.939	1.59	204.93	162.38	[40]	[40]
Hydrogen Chloride	324.55	8.263	11.272	131.4	36.461	[41]	[53]
Hydrogen Sulfide	373.1	9.0	10.19	187.7	34.081	[27]	[60]
Methanol	512.6	8.104	8.6	175.61	32.042	[42]	[61]
Nitrogen	126.19	3.396	11.184	63.151	28.013	[43]	[52]
Octamethylcyclotetrasiloxane	586.5	1.347	1.043	290.25	296.62	[44]	[44]
Oxygen	154.58	5.043	13.63	54.361	31.999	[45]	[52]
Phosgene	462.88	6.459	5.592	145.37	98.916	[46]	[53]
Propylene	364.21	4.555	5.457	87.953	42.08	[11]	[52]
Propyne	402.38	5.626	6.113	170.5	40.06	[47]	[52]
Sulfur Dioxide	430.64	7.884	8.195	197.7	64.064	[27]	[57]
Toluene	591.75	4.126	3.169	178.0	92.138	[27]	[53]
Water	647.1	22.064	17.874	273.16	18.015	[48]	[62]
1,1,1,2,3,3,3-Heptafluoropropane	374.9	2.925	3.495	146.35	170.03	[49]	[63]

within symbol size.

For the ideal gas, all derivatives of the residual Helmholtz energy A^r_{mn} disappear in Eq. (7). With $c^o_v/R = -A^o_{20}$ and $R = c^o_p - c^o_v$ the Grüneisen parameter for the ideal gas is given by the simple relation

$$\gamma_{\mathrm{G}}^{\mathrm{o}} = \frac{c_p^{\mathrm{o}}}{c_v^{\mathrm{o}}} - 1 \,, \tag{8}$$

where c_v^{o} denotes the corresponding isochoric heat capacity. $\gamma_{\mathrm{G}}^{\mathrm{o}}$ isochores were omitted in the figures because they are indistinguishable from the simulation results at the lowest considered density for most investigated substances.

According to their molecular shape, polarity, and hydrogen bonding characteristics, the behavior of γ_{G} is discussed for the various substances in the following subsections. However, some general statements about the (ρ, T) behavior of γ_{G} should be given upfront. The analysis of all 28 fluid systems clearly shows that the Grüneisen parameter γ_{G} strongly depends on both density *and* temperature, which is contrary to the behavior of most solids. The overall dependence of γ_{G} in the fluid phase can be discussed in two different state regions. Outside of the vicinity of the critical point and the gas phase at low temperatures, the Grüneisen parameter increases with increasing density and decreases with increasing temperature. This is a general trend for all fluids except for water. Superimposed to this behavior is the critical region. The Grüneisen parameter approaches zero at the critical point[2] in analogy to the speed of sound.

The Grüneisen parameter may be characterized by a span of minimum and maximum values $(\gamma_{\mathrm{G,\,min}}^{\mathrm{sim}}, \gamma_{\mathrm{G,\,max}}^{\mathrm{sim}})$ to allow for a comparison between different substances. Considering a limited number of substances as investigated by Arp et al.[2], it was stated that γ_G lies in a range from the ideal gas value up to about 2 for most homogeneous fluids. In the present simulation study, we find values deviating up to 80%, i.e. $\gamma_{\mathrm{G,\,max}}^{\mathrm{sim}} = 0.387$ for octamethylcyclotetrasiloxane. To allow for more precise statements, the $(\gamma_{\mathrm{G,\,min}}^{\mathrm{sim}}, \gamma_{\mathrm{G,\,max}}^{\mathrm{sim}})$ spans are collected in Table 2. Because some of the considered EOS are not valid at higher liquid state densities, the spans were determined on the basis of γ_{G} simulation data. The largest

simulated density $\rho_{\mathrm{max}}^{\mathrm{sim}}$ is close to the triple point density for all substances.

In order to concentrate on the essential aspects in the present study, 15 fluids are not detailed in the main part of the paper. Instead, they are collected in the supplementary material[26].

A. Spherical, non-polar molecules

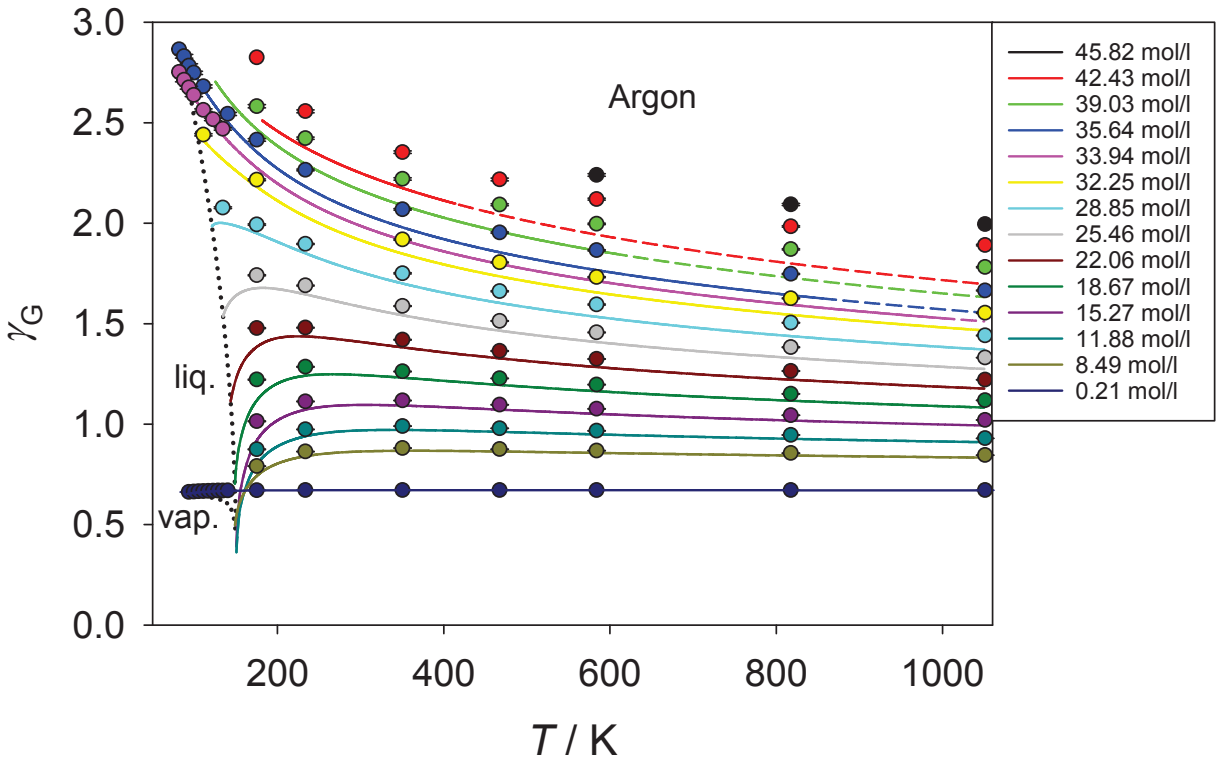

FIG. 1. Grüneisen parameter γ_{G} of argon as a function of temperature along different isochores ranging from $\rho = 0.21$ to 45.82 mol/l.

In Fig. 1 we start with the discussion of γ_{G} for argon, which is one of the most frequently analyzed fluids. Excluding the critical region, the lowest simulated value of $\gamma_{\mathrm{G,\,min}}^{\mathrm{sim}} = 0.671$ occurs at $(\rho_{\mathrm{min}}^{\mathrm{sim}}, T_{\mathrm{max}}^{\mathrm{sim}}) = (0.21 \text{ mol/l}, 1051 \text{ K})$, whereas the largest simulated value of

$\gamma_{\mathrm{G,\,max}}^{\mathrm{sim}} = 2.865$ occurs at $(\rho_{\mathrm{max}}^{\mathrm{sim}}, T_{\mathrm{min}}^{\mathrm{sim}}) = (35.64\ \mathrm{mol/l},\ 81.75\ \mathrm{K})$. According to this scheme, values for all studied fluids are collected in Table 2. Note that $\gamma_{\mathrm{G,\,max}}^{\mathrm{sim}} = 2.865$ is almost 45% above the specified range of values indicated by Arp et al.[2]. At higher densities larger deviations between simulated and EOS values can be observed. The approach of γ_{G} towards zero near the critical point is nicely indicated by both calculation methods.

B. Linear, quadrupolar molecules

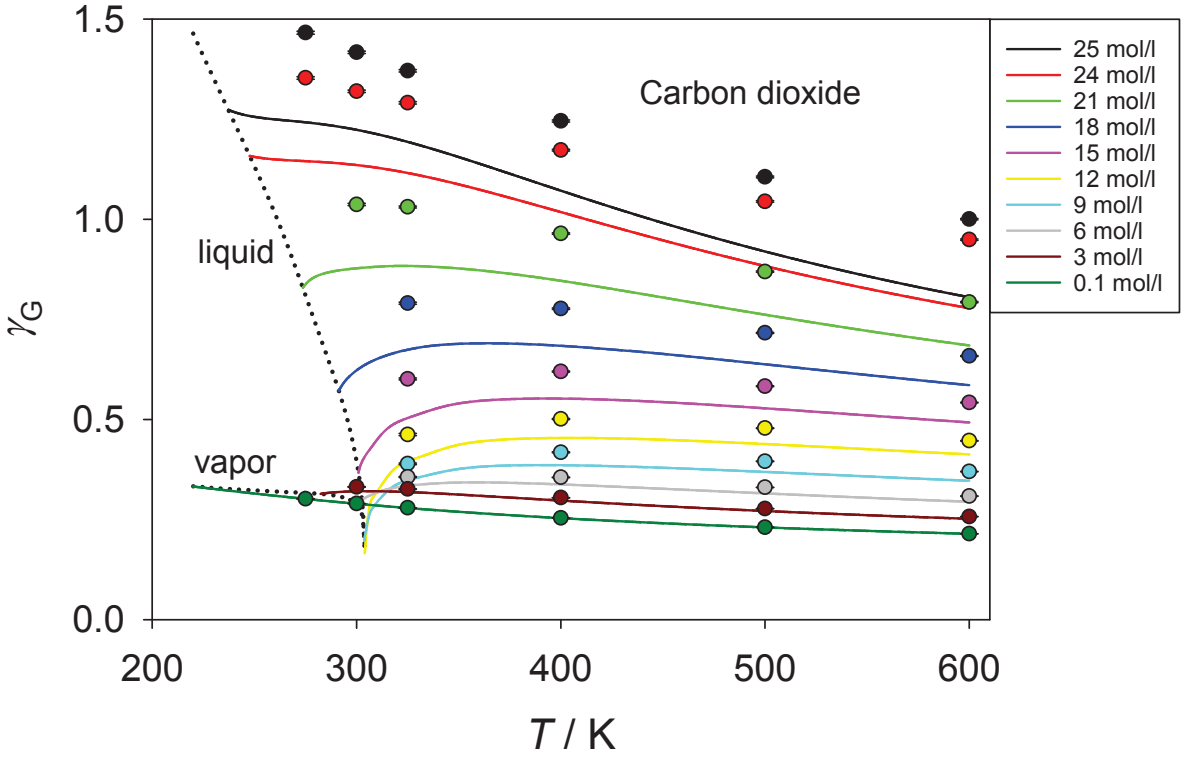

FIG. 2. Grüneisen parameter γ_{G} of carbon dioxide as a function of temperature along different isochores ranging from $\rho = 0.1$ to 25 mol/l.

In this section we discuss the Grüneisen parameter for fluids consisting of linear, quadrupolar molecules. Fig. 2 shows γ_{G} of carbon dioxide as a function of temperature

TABLE II. Range of minimum and maximum values of the Grüneisen parameter γ_{G} obtained from present simulations. No values are included in the table for water because it does not fit into the scheme. Moreover, the results are assigned to different groups (A, B or C) according to their quality as explained in the text.

Substance	$\frac{\rho_{\mathrm{min}}^{\mathrm{sim}}}{\mathrm{mol/l}}$	$\frac{T_{\mathrm{max}}^{\mathrm{sim}}}{\mathrm{K}}$	$\gamma_{G,\,\mathrm{min}}^{\mathrm{sim}}$	$\frac{\rho_{\mathrm{max}}^{\mathrm{sim}}}{\mathrm{mol/l}}$	$\frac{T_{\mathrm{min}}^{\mathrm{sim}}}{\mathrm{K}}$	$\gamma_{G,\,\mathrm{max}}^{\mathrm{sim}}$	A	B	C
Acetone	0.1	800	0.062	14	400	0.82	×		
Ammonia	0.1	800	0.183	40	300	1.255			
Argon	0.21	1051	0.671	35.64	81.75	2.865		×	
Benzene	0.1	1000	0.042	11	400	0.93			
Carbon Dioxide	0.1	600	0.215	25	275	1.466		×	
Carbon Monoxide	0.1	210	0.402	28	100	1.856	×		
Chlorobenzene	0.1	1000	0.041	10.5	275	1.754			
Cyclohexane	1.0	700	0.044	9	340	0.835	×		
Dimethylether	0.1	750	0.075	17	300	1.163			
Ethane	0.1	600	0.104	19	225	1.618	×	×	
Ethanol	0.1	900	0.066	18	375	0.735			×
Ethylene	0.1	600	0.135	22	200	1.826	×		
Ethylene Oxide	0.1	1000	0.079	20	350	1.046	×		
Fluorine	0.1	350	0.349	42	100	2.365			×
Hexamethyldi-siloxane	0.1	1200	0.018	5	300	0.694	×		
Hydrogen Chloride	0.1	400	0.4	33	225	1.532	×		
Hydrogen Sulfide	0.2	400	0.309	30	250	1.698			
Methanol	0.1	900	0.11	28	375	0.804			×
Nitrogen	0.1	275	0.402	29	110	1.909	×	×	
Octamethylcyclo-tetrasiloxane	0.1	1200	0.012	3.2	475	0.387	×		
Oxygen	0.1	300	0.4	36	100	2.127			
Phosgene	0.2	700	0.132	16.2	250	1.985	×		
Propylene	0.1	700	0.076	14	275	1.039	×		
Propyne	0.1	700	0.093	16	300	1.083			×
Sulfur Dioxide	0.1	750	0.193	20	350	1.092	×		
Toluene	0.1	950	0.035	9	475	0.65			
Water	-	-	-	-	-	-		×	
1,1,1,2,3,3,3-Heptafluoropropane	0.1	750	0.043	10	275	0.925	×		

along different isochores. The agreement of the present simulation results with values from the according EOS is reasonable in the gas phase up to the critical density of 10.625 mol/l, whereas in the liquid phase the deviations increase with increasing density. In accordance

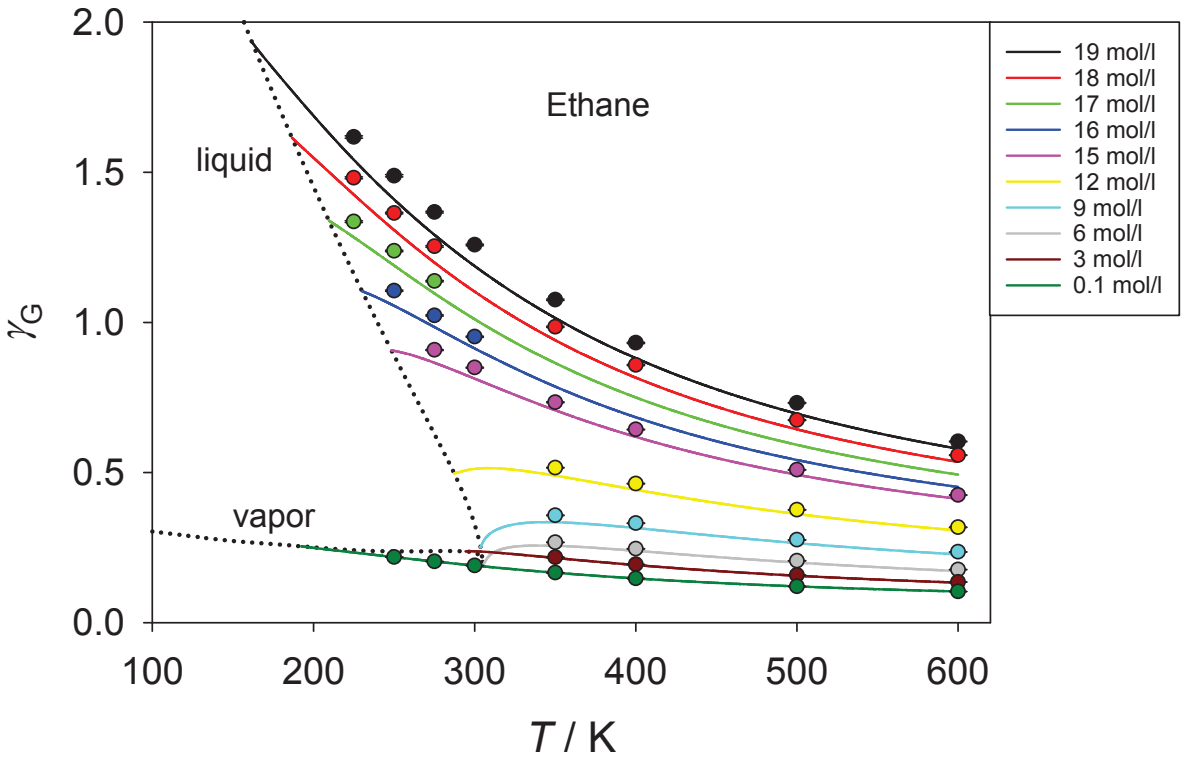

FIG. 3. Grüneisen parameter γ_G of ethane as a function of temperature along different isochores ranging from $\rho = 0.1$ to 19 mol/l.

with the considerations of Arp et al.[2], γ_G isochores bend downwards in the critical region. However, because the present simulation data do not cover the vicinity of the critical point the approach of γ_G to zero can not be demonstrated.

The resemblance between simulation results and EOS values, even in the dense liquid phase, is much better for ethane and ethylene as shown in Figs. 3 and 4. Both substances exhibit a strong temperature dependence at higher densities. Increasing the temperature causes a strong decrease of the Grüneisen parameter, which shows that the assumption of temperature independence in solids is not applicable in the liquid phase.

The Grüneisen parameter γ_G of nitrogen (Fig. 5) follows the general trend discussed

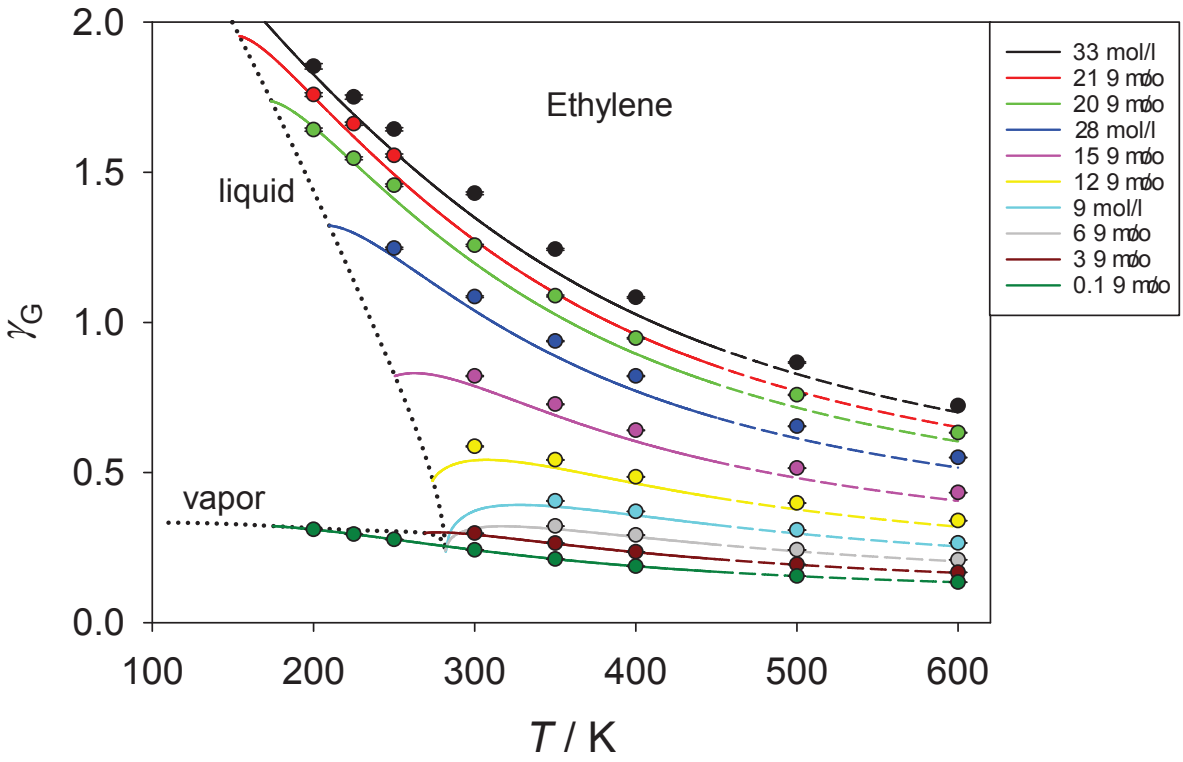

FIG. 4. Grüneisen parameter γ_G of ethylene as a function of temperature along different isochores ranging from $\rho = 0.1$ to 22 mol/l.

above. Comparing simulated γ_G values with those calculated from the corresponding EOS shows that larger deviations can be observed at high densities and high temperatures.

Fluorine, oxygen, propyne and propylene also belong to the class of linear, quadrupolar fluids and are discussed in the supplementary material[26].

C. Triangular, dipolar molecules

As representatives for triangular, dipolar molecules, we discuss here the state dependence of the Grüneisen parameter of acetone, ethylene oxide and phosgene. Dimethylether and sulfur dioxide are discussed in the supplementary material[26]. Fig. 6 presents the γ_G tem-

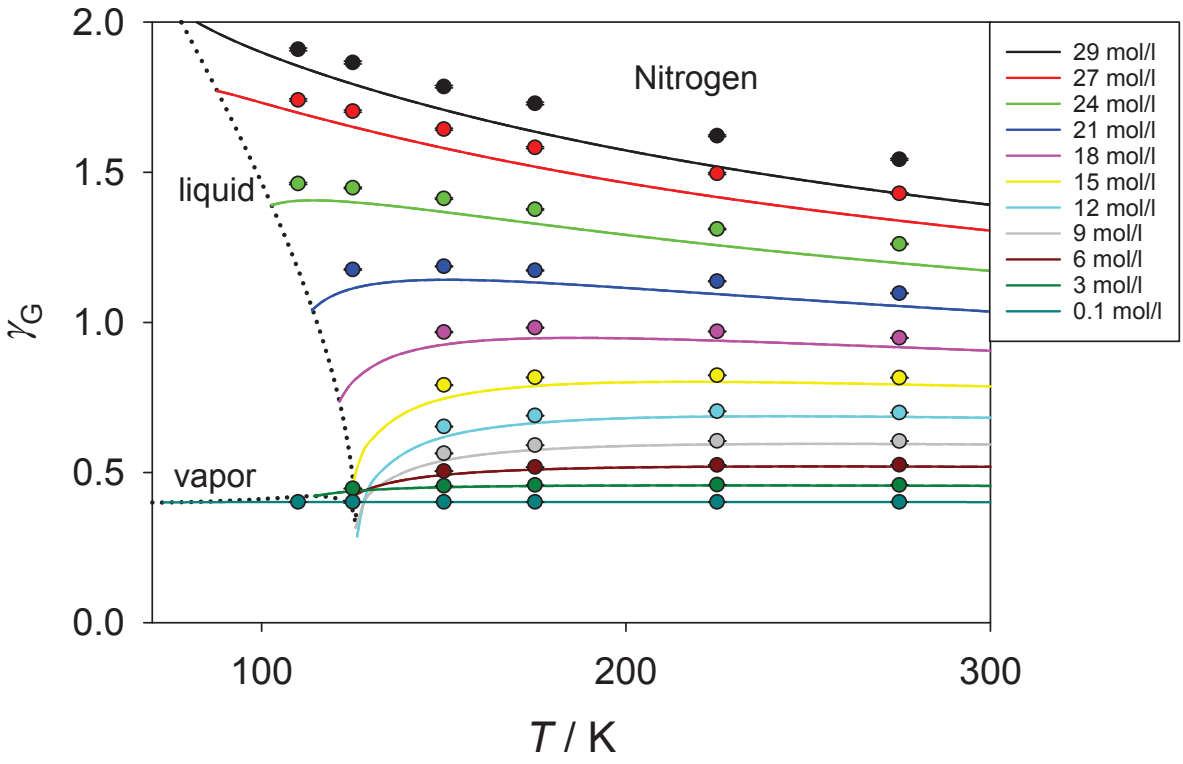

FIG. 5. Grüneisen parameter γ_G of nitrogen as a function of temperature along different isochores ranging from $\rho = 0.1$ to 29 mol/l.

perature dependence of acetone along isochores with a good agreement between simulated and EOS data.

Figs. 7 and 8 present temperature-dependent results of the Grüneisen parameter for ethylene oxide and phosgene, respectively. For ethylene oxide, the applied EOS[38] belongs to a new generation of EOS because it was correlated to a hybrid data set (experimental and molecular simulation data)[64]. The reactive nature of ethylene oxide makes this substance particularly hazardous: it is carcinogenic, mutagenic, and highly flammable at room temperature. It is thus not surprising that the availability of experimental data is very limited. Experimental data cover almost exclusively the gaseous phase. Therefore, molecular simu-

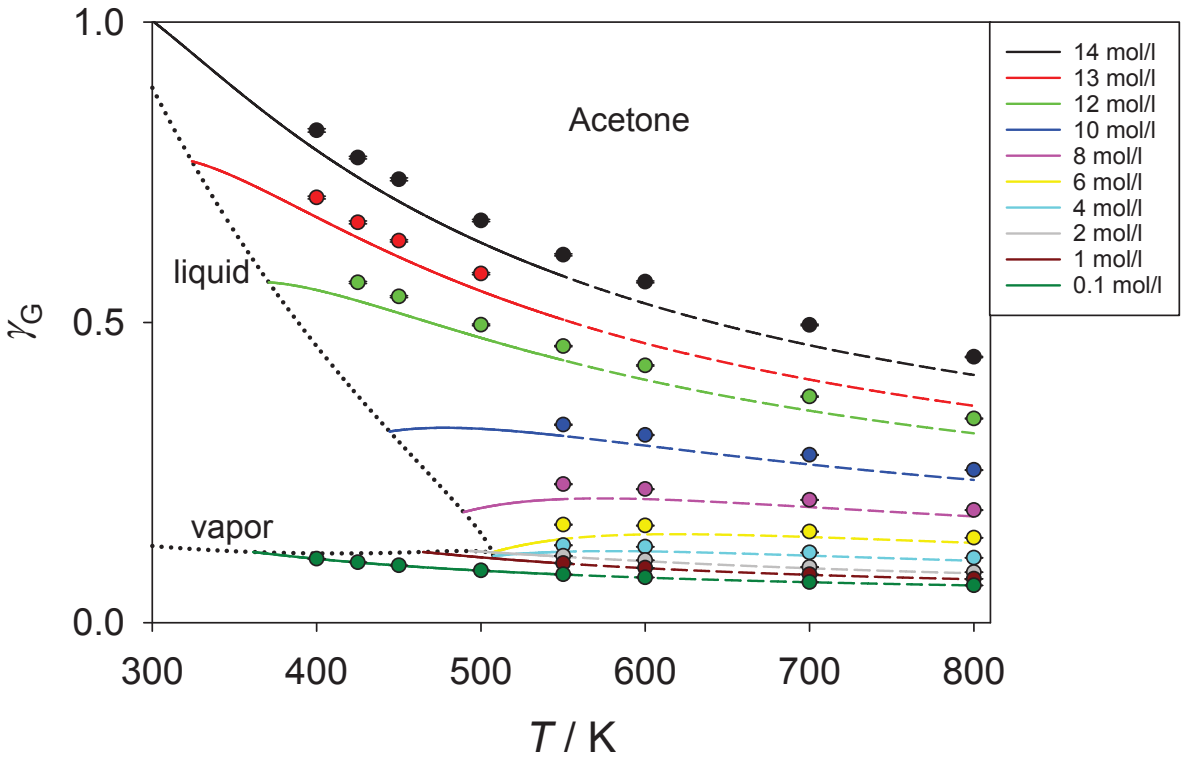

FIG. 6. Grüneisen parameter γ_G of acetone as a function of temperature along different isochores ranging from $\rho = 0.1$ to 14 mol/l.

lation data were used to extend the validity of the EOS to the liquid state because elevated temperatures or pressures are not limiting factors for molecular simulation. Fig. 7 shows that up to a density of $\rho = 16$ mol/l the correspondence between the EOS and simulation data is good, for $\rho \geq 18$ mol/l some deviations can be seen. Near the critical point, γ_G obtained from the EOS suggests an approach to zero, whereas the simulation results do not show this tendency, presumably because the number of particles used in the simulations was not large enough.

For phosgene, the situation is similar as for ethylene oxide. Due to its hazardous and extremely toxic nature, laboratory measurements are hardly available or very old. Therefore,

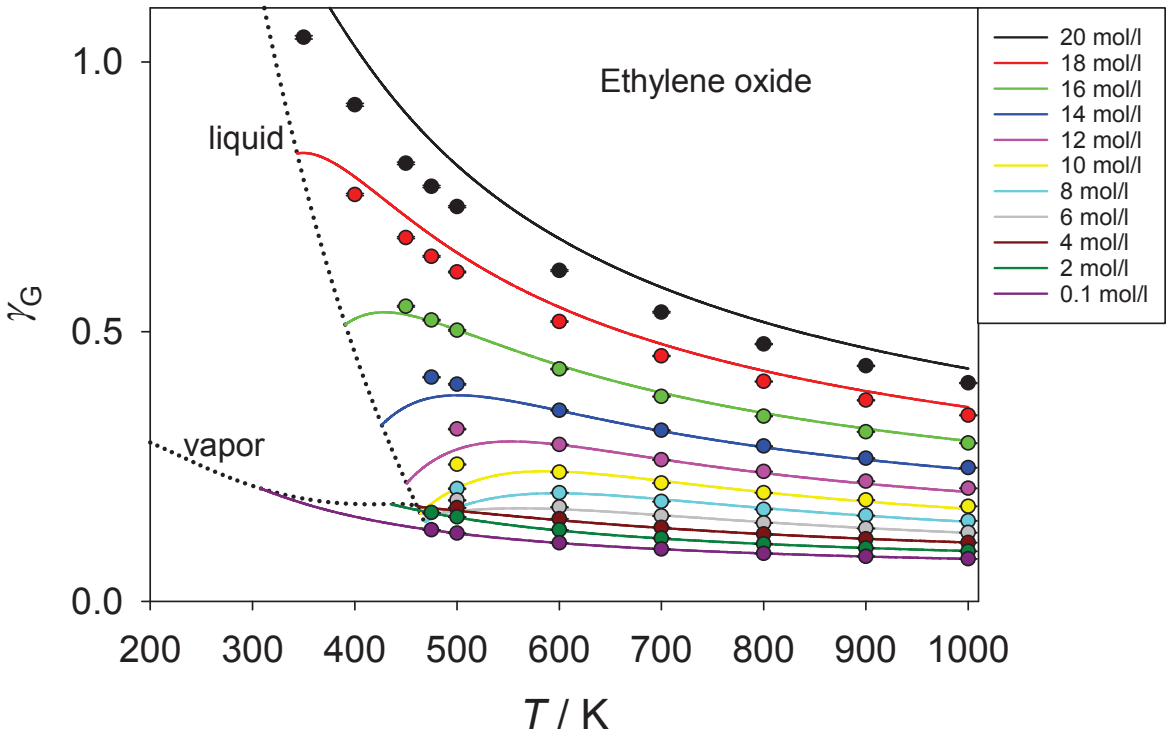

FIG. 7. Grüneisen parameter γ_G of ethylene oxide as a function of temperature along different isochores ranging from $\rho = 0.1$ to 20 mol/l.

a modified Benedict-Webb-Rubin (MBWR) type EOS[65] has been developed for phosgene which is solely based on simulation data[46]. The correlation procedure was improved with respect to the conventional method. Based on a purely simulated dataset, usually only pressure and energy values are correlated[66]. For phosgene, also higher order Helmholtz energy derivatives according to Eq. (6) have been applied in the correlation procedure. Fig. 8 shows that the agreement between simulation data and EOS results is excellent throughout and, compared to the conventional method, demonstrates fundamental improvements when using this new fitting technique.

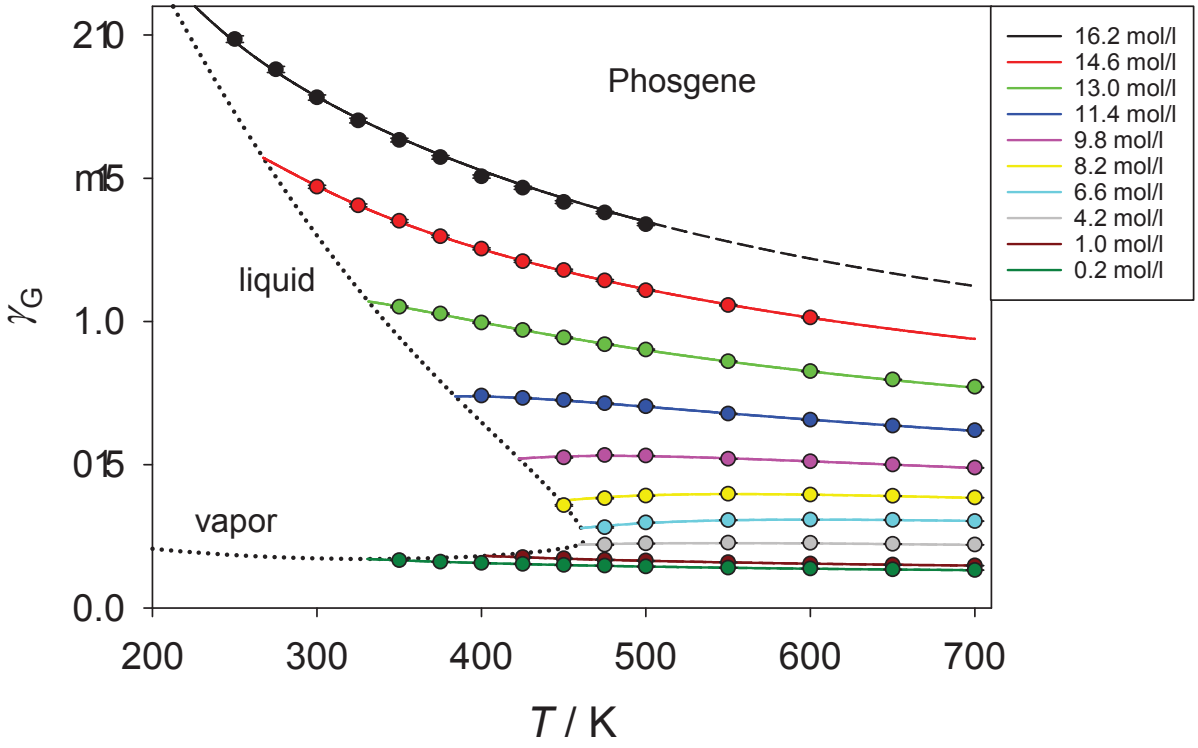

FIG. 8. Grüneisen parameter γ_G of phosgene as a function of temperature along different isochores ranging from $\rho = 0.2$ to 16.2 mol/l.

D. Hydrogen bonding molecules

Hydrogen bonding fluids are of particular interest in this study because especially water does not follow the general (ρ, T) trend of γ_G.

Fig. 9 shows the (ρ, T) behavior of γ_G of hydrogen chloride. From a chemical perspective real hydrogen chloride is not considered as a hydrogen bonding fluid. Its molecular model, however, is constructed in the same qualitative way as those for hydrogen bonding fluids (like water or methanol), i.e. employing point charges that are eccentrically superimposed to a Lennard-Jones site. Therefore, it is discussed in this section. The agreement between simulated and EOS data is reasonably well, especially in the high density and high tempera-

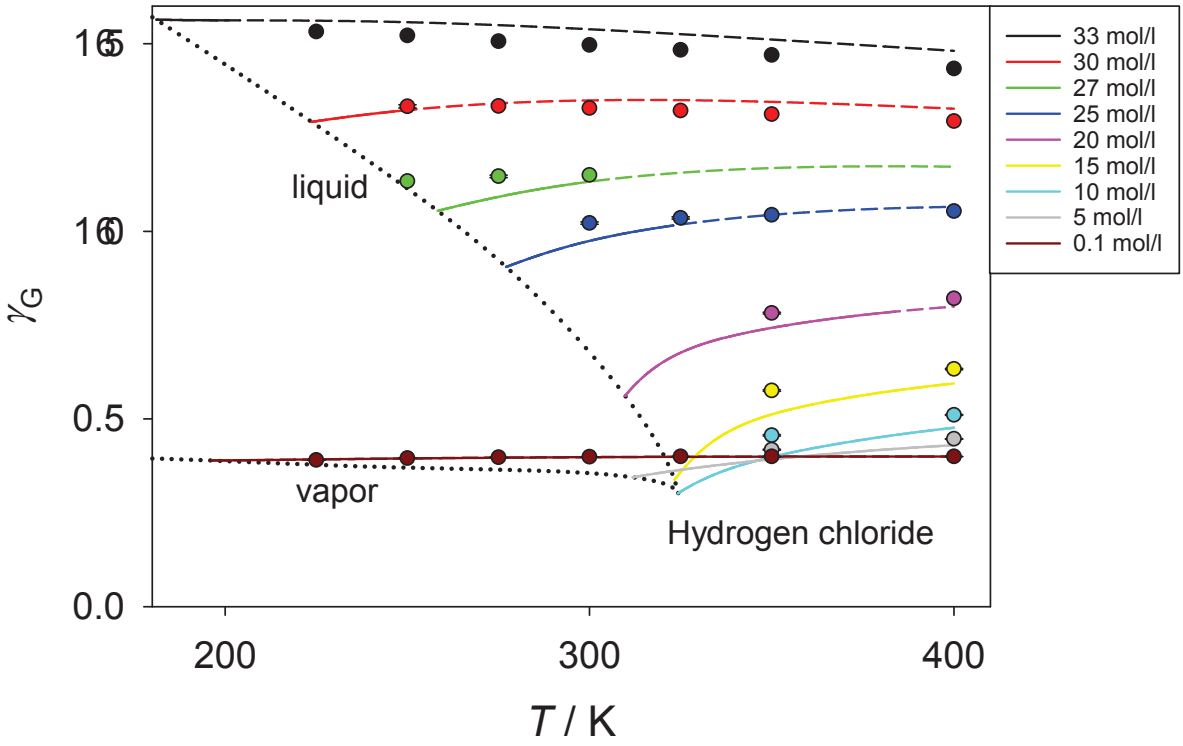

FIG. 9. Grüneisen parameter γ_G of hydrogen chloride as a function of temperature along different isochores ranging from $\rho = 0.1$ to 33 mol/l.

ture region, where only extrapolations of the EOS (dashed lines) were used. The interesting point in case of hydrogen chloride is that this substance is the only one in the present study, in which the γ_G isochores are roughly independent on temperature at higher densities.

The Grüneisen parameter of water, shown in Fig. 10, behaves very exceptional compared with all other fluids discussed here. The γ_G isochores in stable states from EOS are based on the IAPWS-95 formulation[48], an equation with a very high level of accuracy, sometimes called reference quality EOS (see discussion in section 3.8). γ_G isochores, calculated from this equation, exhibit a maximum in the supercritical region at high densities, e.g. at a density of $\rho = 58$ mol/l the maximum occurs at $T = 657$ K slightly above the critical temperature

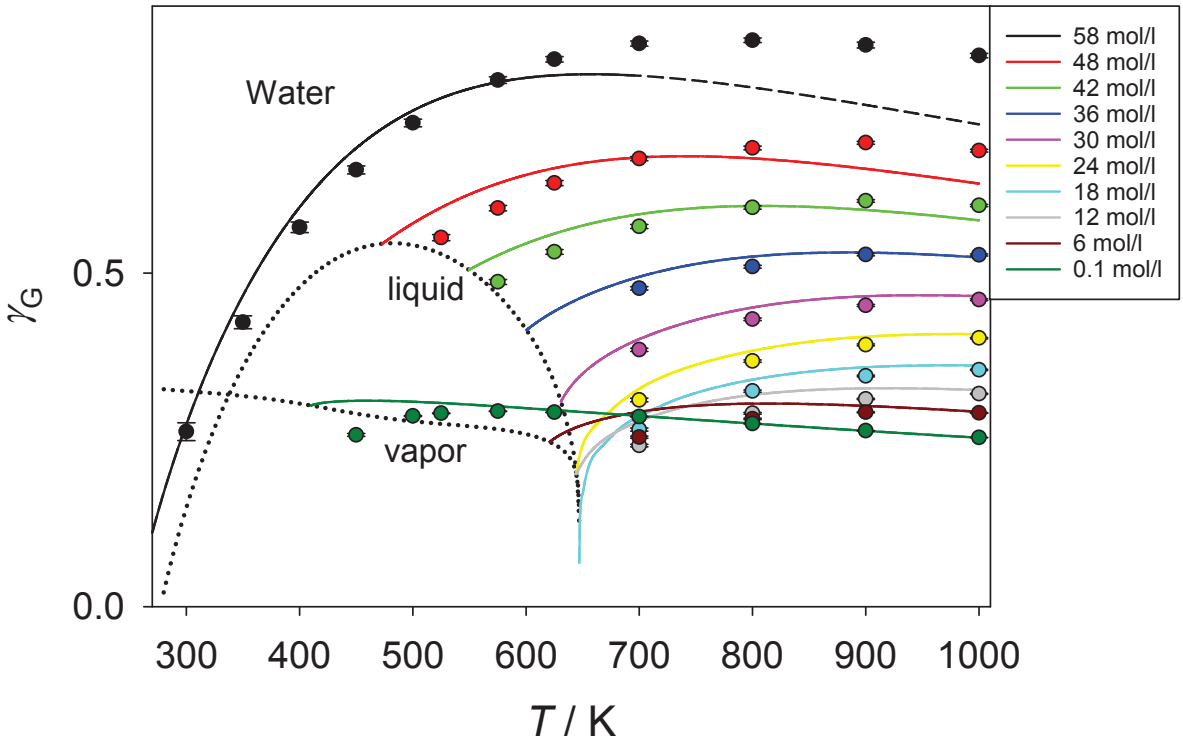

FIG. 10. Grüneisen parameter γ_G of water as a function of temperature along different isochores ranging from $\rho = 6$ to 58 mol/l.

of $T_c = 647.1$ K. Furthermore, γ_G develops a maximum along the liquid saturation line at a temperature of $T \approx 480$ K. Decreasing the temperature further causes a crossing of γ_G along the liquid and vapor saturation line at a temperature of $T \approx 338$ K. In the dense liquid state at low temperatures, γ_G drops sharply and even becomes negative (not shown in Fig. 10), which is contrary to all other fluids in this study. The simulation results, performed with the TIP4P/2005 interaction model[62], only show a good agreement with the IAPWS-95 EOS at a high density of 58 mol/l and low temperatures as well as on the liquid side of the supercritical region in a range of $24 < \rho$ / mol/l < 42. However, maxima are also present along the simulated isochores at high densities which, compared with the IAPWS-95 EOS,

are shifted to higher temperatures, e.g. at $\rho = 58$ mol/l to a temperature of $T \approx 800$ K.

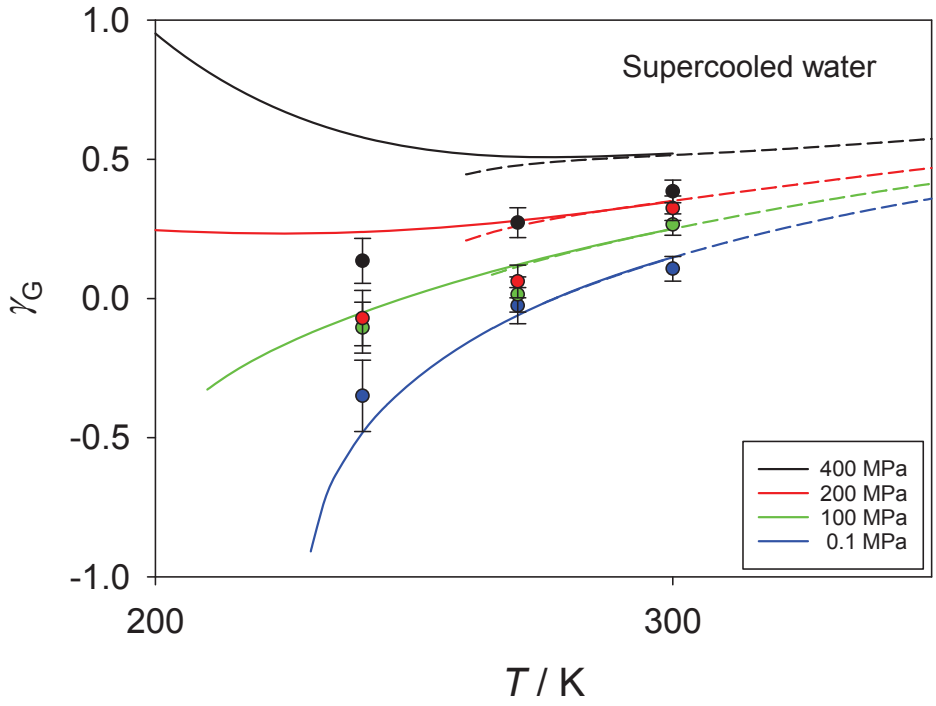

FIG. 11. Grüneisen parameter γ_G of supercooled water as a function of temperature along different isobars ranging from $p = 0.1$ to 400 MPa. Solid lines represent the TSEOS of Holten *et al.*[67] and dashed lines the IAPWS-95 EOS[48].

Negative values of γ_G can easily be explained by looking at the first expression in Eq. (3). The isothermal compressibility β_T and the isochoric heat capacity c_v are always positive in the entire single-phase fluid region, whereas the thermal expansion coefficient α_p shows anomalous behaviour when it becomes negative. Therefore, all fluids having a density anomaly show negative values of γ_G which occurs for water at $T = 277$ K and ambient pressure. An equivalent behavior could be demonstrated e.g. for the Gaussian core model fluid[7]. As a consequence of a negative thermal expansion coefficient, a strongly decreasing γ_G to negative values can be demonstrated more clearly in the supercooled region (Fig. 11). The Grüneisen parameter of supercooled water was evaluated with a two-state equation of

state (TSEOS) correlated to the most recent experimental data. The TSEOS was developed by Holten *et al.*[67] to model the anomalous behavior of several thermodynamic properties of metastable supercooled water. Holten *et al.*[67] assumed that liquid water at low temperatures can be described as a mixture of two interconvertible states of local molecular order, namely a high-density liquid (HDL) and a low-density liquid (LDL) whose ratio is controlled by thermodynamic equilibrium. It is believed that the competition between these two configurations generates the anomalies of the thermodynamic properties of cold and supercooled water. The model assumes a liquid-liquid (HDL-LDL) critical point at $\rho_c = 914.84$ g/l, $T_c = 228$ K and $p_c = 0$ MPa and was fitted to experimental data ranging from the homogeneous ice nucleation temperature up to 300 K for pressures below 400 MPa. Because it is formulated in terms of the Gibbs energy as an implicit function of temperature and pressure, the temperature dependence of the Grüneisen parameter is discussed in Fig. 11 along isobars. The solid lines represent γ_G isobars obtained from the TSEOS covering a range from roughly -1 near the assumed liquid-liquid critical point to +1 at a pressure of $p = 400$ MPa and low temperaures. The change to negative γ_G values occurs at a pressure of about 150 MPa in accordance with the appearance of the expansivity anomaly at this pressure[68]. In the supercooled region, additional simulations were performed with the TIP4P/2005 potential model. Compared with the stable liquid state, larger statistical fluctuations are present in the metastable, supercooled state. However, within the error bars a reasonable agreement with the TSEOS can be observed up to a pressure of $p = 100$ MPa. For pressures $p > 150$ MPa large deviations exist between simulation data and TSEOS results.

It is of some interest to compare the behavior of the Grüneisen parameter obtained from the TSEOS model with the IAPWS-95 formulation[48] close to the melting line. γ_G isobars obtained from the IAPWS-95 EOS are shown as dashed lines in Fig. 11. Both curves

exhibit a smooth connection without significant discontinuities at the point of switching. When extrapolating the data from the IAPWS-95 formulation into the supercooled region at $p = 0.1$ MPa, the Grüneisen parameter follows closely that of the TSEOS. An increase in pressure results in decreasing compliance at low temperatures. This is a result that confirms the findings made in the analysis of the thermodynamic curvature scalar for both EOS[69,70].

Note that ammonia, ethanol, methanol and hydrogen sulfide as additional hydrogen bonding fluids are discussed in the supplementary material[26].

E. Cyclic molecules

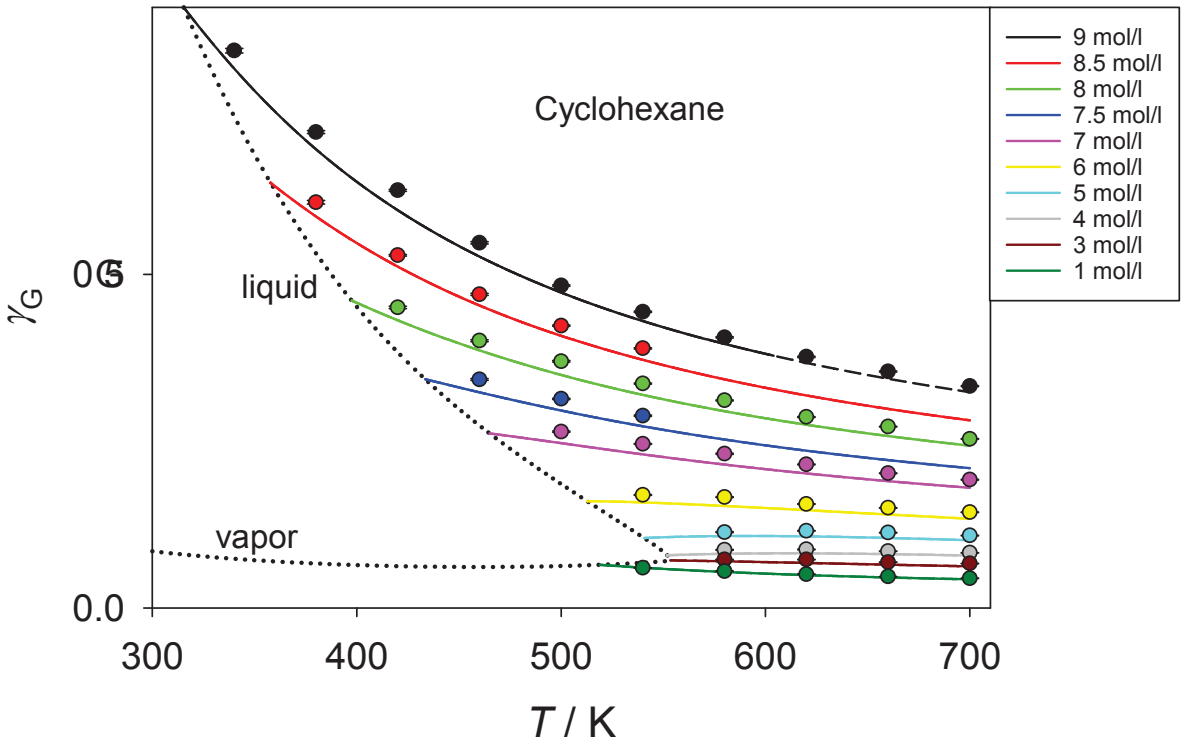

FIG. 12. Grüneisen parameter γ_G of cyclohexane as a function of temperature along different isochores ranging from $\rho = 1$ to 9 mol/l.

As an example for a cyclic molecule, the Grüneisen parameter of cyclohexane is presented in Fig. 12. γ_G follows the general (ρ, T) trend and the agreement between simulation and EOS results is satisfactory. Benzene, chlorobenzene and toluene as additional cyclic molecules are discussed in the supplementary material[26].

F. Siloxanes

Siloxanes are considered as an important group of working fluids in heat recovery systems, such as organic Rankine cycles (ORC). They possess an excellent thermal and chemical stability and are not toxic. In addition, siloxanes are possible candidates for *BZT* fluids mentioned above[71]. Therefore, two siloxanes are discussed in this paper, namely hexamethyldisiloxane (Fig. 13) and octamethylcyclotetrasiloxane, given in the supplementary material[26]. Particularly hexamethyldisiloxane appears to be a good candidate for becoming a widely employed working fluid for high-temperature ORC processes. In order to extend the existing experimental data of hexamethyldisiloxane particularly to higher temperatures, additional simulations were performed in Ref.[40]. A new EOS was developed[40] based on this hybrid data set similar to the method that was used for ethylene oxide. As in the case of ethylene oxide and phosgene, this extended fitting strategy allows for the determination of an EOS with a high accuracy. The temperature-dependent behavior of the Grüneisen parameter is presented in Fig. 13.a. An excellent agreement can be observed between simulated and EOS data.

It is our intention to determine the fundamental derivative of gas dynamics Γ[72] according to Eq. (4) in a future project for the two siloxanes discussed in this study. The region of interest for a *BZT* fluid is the single-phase vapor region. In Fig. 13.b the density-dependent behavior of γ_G in this region is presented for isotherms up to a temperature of $T = 523.15$

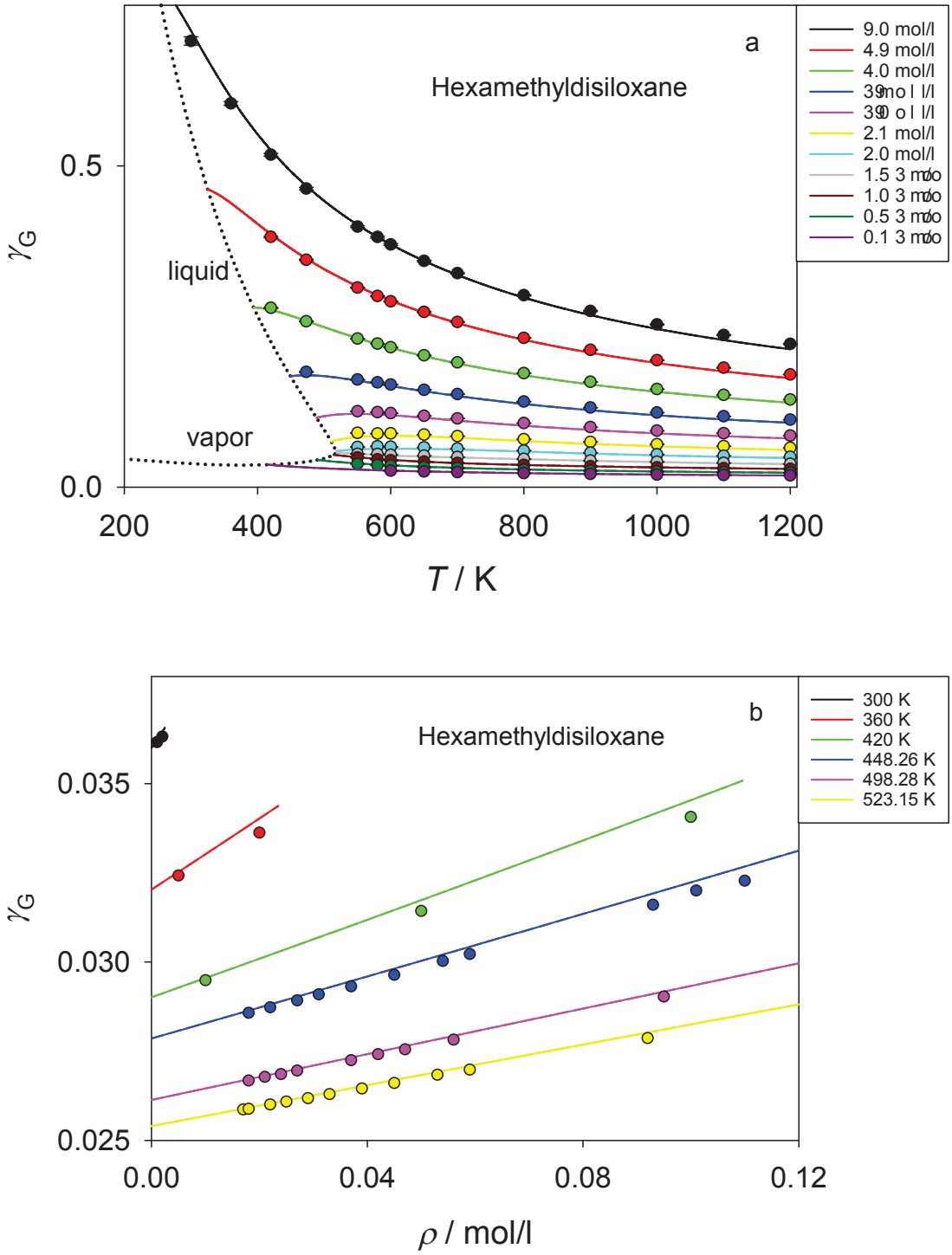

FIG. 13. Grüneisen parameter γ_G of hexamethyldisiloxane as a function of temperature (a) along different isochores ranging from $\rho = 0.1$ to 5 mol/l and as a function of density (b) on the vapor side along different isotherms ranging from $T = 300$ to 523.15 K.

K slightly above the critical temperature of $T_c = 518.75$ K. Again, the agreement between simulated and EOS data is good, which should allow for a reliable determination of Γ.

G. Other fluids

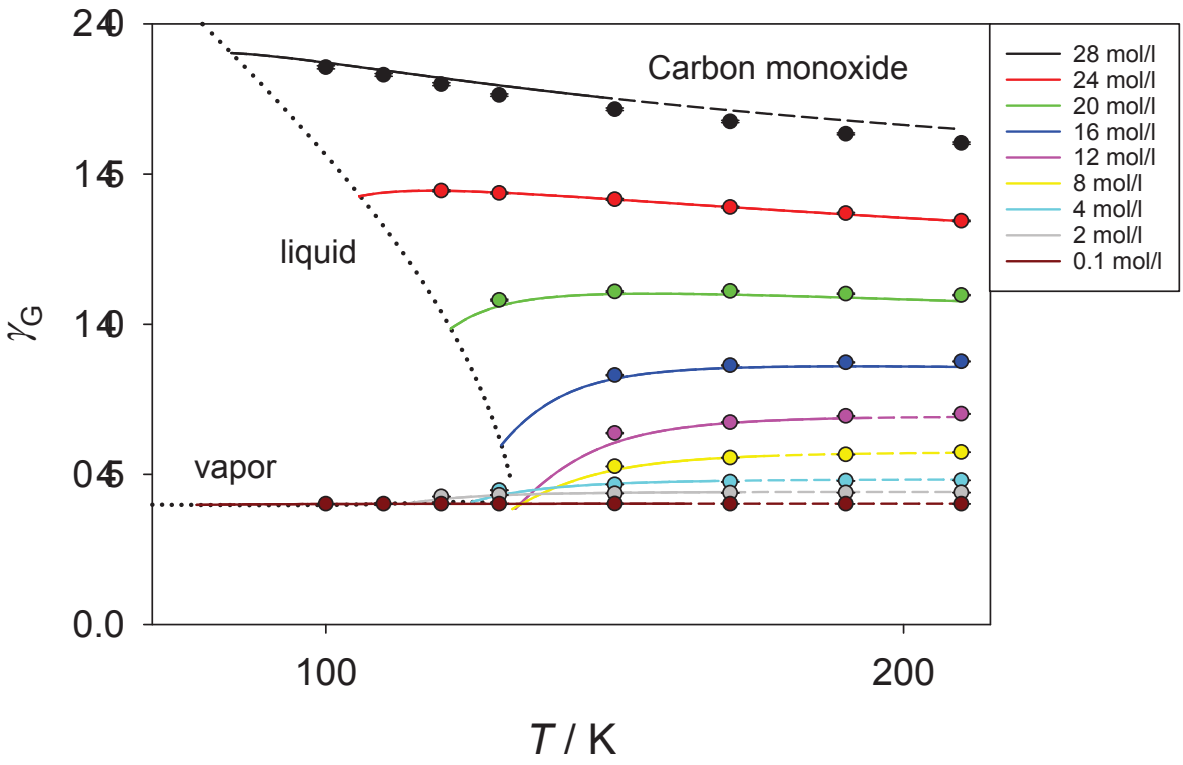

FIG. 14. Grüneisen parameter γ_G of carbon monoxide as a function of temperature along different isochores ranging from $\rho = 0.1$ to 28 mol/l.

In this final section, we discuss the remaining fluids which do not really belong to the previous sections. The Grüneisen parameter of carbon monoxide is shown in Fig. 14 with a good agreement between simulation and EOS data. The phase behavior of the Grüneisen parameter of 1,1,1,2,3,3,3-Heptafluoropropane (C_3HF_7) is presented in the supplementary material[26].

H. Simulation versus EOS results

For a certain number of fluids, deviations occur between simulation results and the values obtained from the according EOS. For some EOS especially at high densities, only their extrapolated values could be used for comparison because experimental data were limited or not available in this state region. In turn, also the molecular interaction models will not always be optimal in any particular phase region. Therefore, it is of interest to review the simulation results against the EOS data. Proceeding in this direction, the outcomes of the 28 studied fluids are assigned to three groups as summarized in Table 2.

Group A contains all fluids with a good or at least satisfactory agreement between simulation and EOS results.

The second, very important, group B collects all fluids which are privileged to have their own reference quality EOS as defined by Span[23]. The construction of this type of EOS requires a large amount of experimental data, months or years of careful data filtering and complex non-linear fitting. Only a very limited number of fluids (less than ten) have a reference quality EOS such as argon, carbon dioxide, ethane, nitrogen or water. The simulations for argon (Fig. 1) were performed on the basis of the classical Lennard-Jones potential. One weakness of this potential is the lack of a realistic description of repulsion, which originates from the Pauli exclusion principle. It might be of interest to examine whether the deviations in the Grüneisen parameter at high density and temperature between simulation and EOS data are caused by this issue. Likewise, the molecular interaction model of carbon dioxide (Fig. 2) can not reproduce results of the corresponding reference quality EOS at high densities. For water (Fig. 10), the simulation results, based on the TIP4P/2005 interaction model[62], do not follow the IAPWS-95 reference quality EOS[48] in different regions

of the phase space. As it is well known, the development of an interaction model for water that is valid in a large phase space region continues to be a major challenge[73]. The agreement between simulation and EOS values for ethane (Fig. 3) and nitrogen (Fig. 5) is satisfactory.

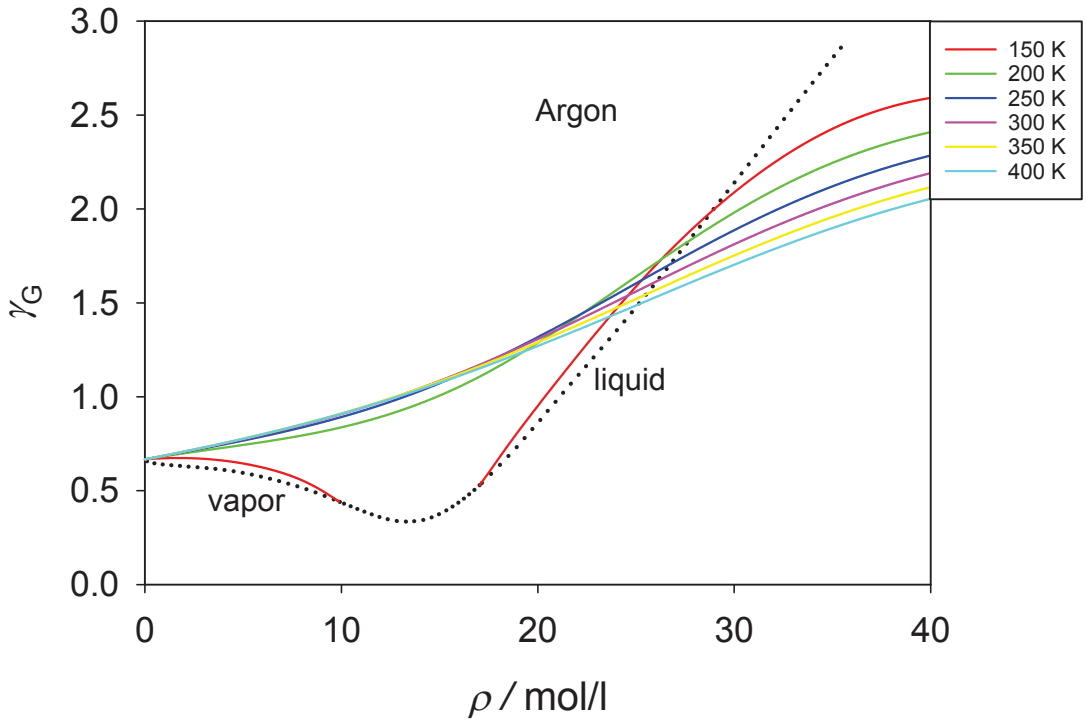

FIG. 15. Grüneisen parameter γ_G of argon as a function of density along different isotherms ranging from $T = 150$ to 400 K obtained from the EOS[29].

Recently, the use of the Grüneisen parameter was suggested to verify the correct qualitative behavior of EOS[11,12]. Because of the identities given in Eq. (3), the behavior of the speed of sound as well as the isochoric and isobaric heat capacities can be simultaneously monitored by the Grüneisen parameter. The assumed qualitatively correct behavior of an EOS can be explained in the density-dependent representation of γ_G along isotherms as given, e.g., for argon in Fig. 15. Because of the general (ρ, T) trend explained above, the isotherms at high temperatures show an increasing Grüneisen parameter with increasing

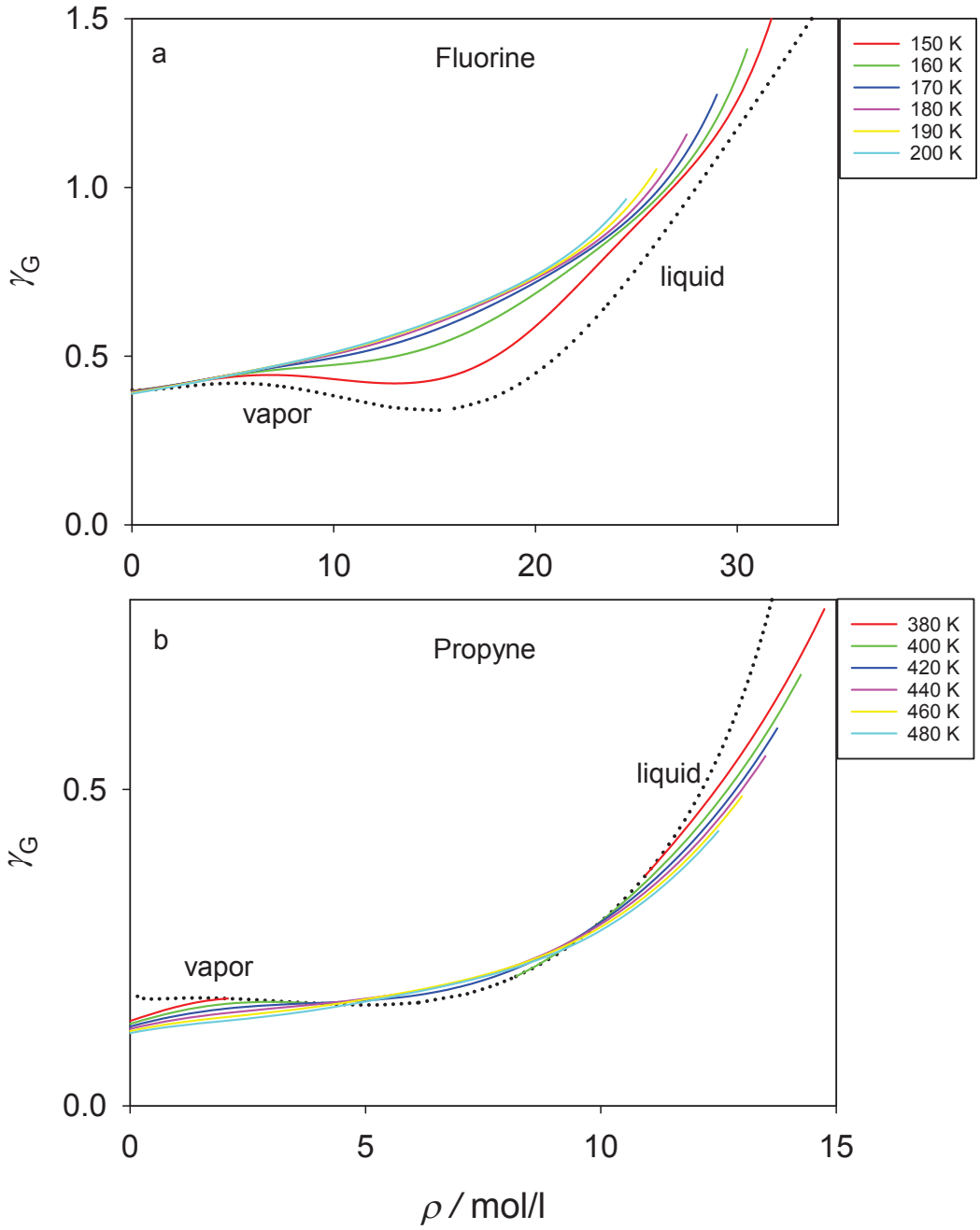

FIG. 16. Grüneisen parameter γ_G as a function of density (a) of fluorine along isotherms ranging from $T = 150$ to 200 K, and (b) of propyne along isotherms ranging from $T = 380$ to 480 K. The γ_G isotherms were obtained from the corresponding EOS. They show two typical cases of deviant behavior of the Grüneisen parameter as described in the text.

density. Due to the superposition of the critical region with an approach to zero at the critical point, a crossing of isotherms must occur beyond the critical density accompanied with a change to negative curvature as already shown in recent work[11,12]. This behavior is assumed to be correct because it was found for several different fluids. Some of the EOS deviate from this behavior. In Fig. 16 we show two typical examples of deviant behavior of the examined EOS. Fig. 16.a presents the Grüneisen parameter of fluorine where no crossing of the isotherms nor a change to negative curvature at higher densities can be seen. The Grüneisen parameter of propyne (Fig. 16.b) shows a crossing of the isotherms, whereas a change to a negative curvature does not occur. All fluids for which the EOS differ in such a way from the presumed behavior are collected in group C as summarized in Table 2. For these fluids, the simulation results are, at least, more plausible.

Seven fluids (amonia, benzene, chlorobenzene, dimethylether, hydrogen sulfide, oxygen and toluene) have not been assigned to the three groups. They exhibit the correct assumed behavior of the associated EOS, but still reveal deviations from the simulation results. It is believed that the thermodynamic behavior of benzene and chlorobenzene is correctly described by their EOS because not only (p, ρ, T) data but also accurate speed of sound data were available during the fitting procedure. For the remaining fluids we have to leave the assessment open.

The maximum values of the simulated Grüneisen parameter $\gamma_{\mathrm{G,\,max}}^{\mathrm{sim}}$ vary between 0.387 for octamethylcyclotetrasiloxane and 2.865 for argon. By interpreting the results of Table 2, it might be natural to deduce, in some way, a correlation between a decreasing Grüneisen parameter and increasing complexity of the molecules. Because of the absence of a general theory, an attempt was made to find empirical correlations between γ_{G} and various substance parameters. For this purpose, it is necessary to compare the 28 fluids at equivalent state

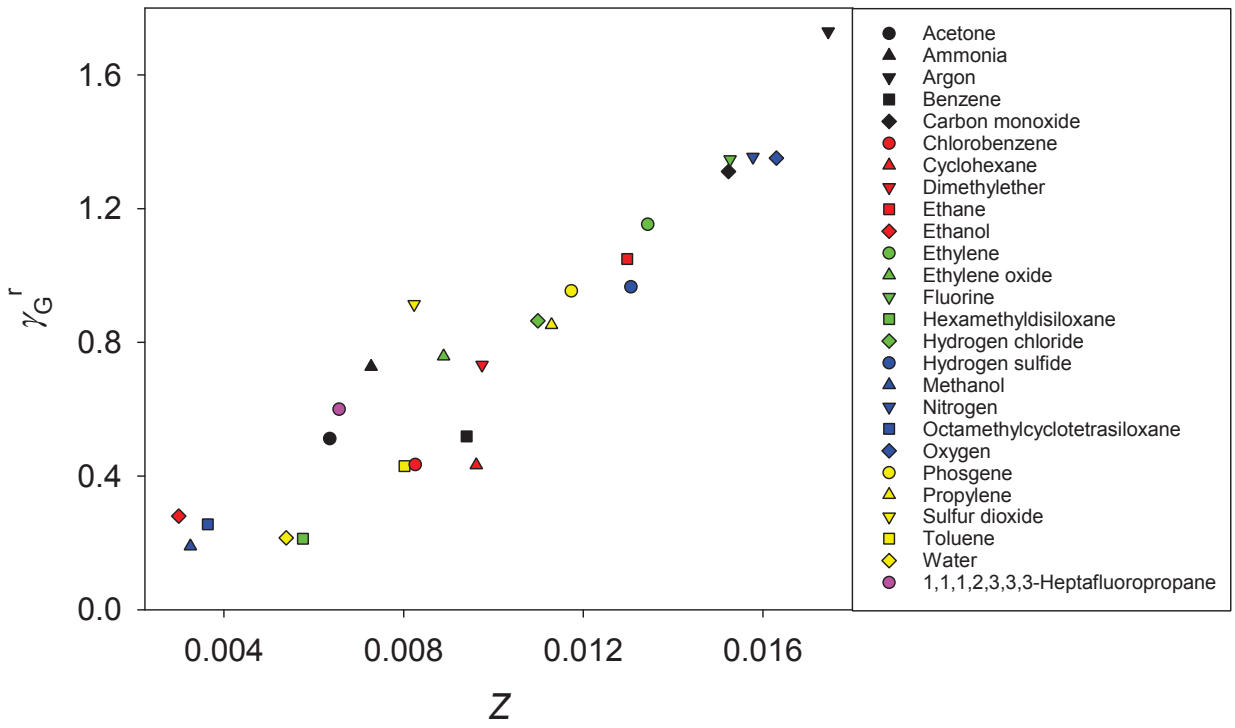

FIG. 17. Residual Grüneisen parameter $\gamma_G^r = \gamma_G - \gamma_G^o$ as a function of compressibility $Z = p/(\rho RT)$ on the corresponding liquid saturation line at $(\rho_{lsat}, 0.7\ T_c)$ for 26 fluids. Carbon dioxide and propyne are not included (see text).

points. Two state points were chosen for comparison, one close to the respective triple points at $(\rho_{tr}, 1.1\ T_{tr})$ and the second one on the corresponding liquid saturation (lsat) line at $(\rho_{lsat}, 0.7\ T_c)$ with $\rho_{lsat} = \rho_{lsat}(0.7\ T_c)$. A temperature of 0.7 T_c is also widely used for the phase characterization of pure components in terms of the acentric factor ω, which is a measure of the non-sphericity of molecules. For both state points, the Grüneisen parameter of all 28 fluids was correlated with different substance parameters (molar weight, molecular degrees of freedom, isochoric heat capacity, compressibility, acentric factor as well as triple point (ρ_{tr}, T_{tr}) and critical data (p_c, ρ_c, T_c)) using both simulated and EOS results. For all these parameters, no strong correlation was found. However, a weak correlation between

the residual Grüneisen parameter $\gamma_{\mathrm{G}}^{\mathrm{r}} = \gamma_{\mathrm{G}} - \gamma_{\mathrm{G}}^{\mathrm{o}}$ and the compressibility $Z = p/(\rho RT)$ on the liquid saturation line at $(\rho_{\mathrm{lsat}}, 0.7\,T_{\mathrm{c}})$ was found, as shown in Fig. 17 for the EOS data. Carbon dioxide and propyne are not included in Fig. 17. For carbon dioxide, $0.7\,T_{\mathrm{c}} < T_{\mathrm{tr}}$. The behavior of γ_{G} of propyne along the vapor-liquid coexistence line is represented poorly by the according EOS (cf. Fig. 16.b), causing a larger error in $\gamma_{\mathrm{G}}^{\mathrm{r}}$. Fig. 17 suggests an almost linear increase of $\gamma_{\mathrm{G}}^{\mathrm{r}}$ with increasing compressibility of the fluid components at $(\rho_{\mathrm{lsat}}, 0.7\,T_{\mathrm{c}})$.

IV. CONCLUSION

The behavior of the Grüneisen parameter γ_{G} was analyzed in detail for 28 pure fluids. We establish that the phase space behavior of γ_{G} for fluids follows a general trend. The Grüneisen parameter increases with increasing density and decreases with increasing temperature, if the critical region is excluded. Therefore, the assumption often used for solids, that γ_{G} is independent of temperature can not be applied to the fluid state. We find exceptions from this general trend for water. Different spans of γ_{G} are characterized by a range of minimum and maximum values. Deviations between simulation results and EOS data, especially at high densities, could be assessed by assigning the outcomes to three different quality groups. In group A all fluids are summarized, providing credible results with respect to the EOS and the simulation. Group B includes all substances whose EOS is preferable to the simulation results. Group C collects all fluids in which the associated EOS leads to an inconsistent thermodynamic behaviour. Here, the simulation results are, at least, more plausible. To the best of our knowledge, this study represents the first detailed analysis of the Grüneisen parameter for a large number of fluids over a very large region of thermodynamic states.

Acknowledgments

The simulations were carried out on the Oculus cluster (PC^2) at the University of Paderborn and the national supercomputer Hazel Hen at the High Performance Computing Center Stuttgart (HLRS) within Project No. MMHBF2.

REFERENCES

[1]N. W. Ashcroft and N. D. Mermin, *Solid State Physics*, Holt-Saunders International Editions (1981).

[2]V. Arp, J. M. Persichetti, and Chen Guo-bang, "The Grüneisen Parameter in Fluids," J. Fluids Eng. **106**, 193-200, (1984).

[3]P. A. Thompson, "A Fundamental Derivative in Gasdynamics," Phys. of Fluids. **14**, 1843-1849, (1971).

[4]P. A. Thompson and K. Lambrakis, "Negative Shock Waves," J. Fluid Mech. **60**, 187-208, (1973).

[5]R. Menikoff and B. J. Plohr, "The Riemann Problem for Fluid Flow of real Materials," Rev. Mod. Phys. **61**, 75-130, (1989).

[6]R. Casalini, U. Mohanty, and C. M. Roland, "Thermodynamic interpretation of the scaling of the dynamics of supercooled liquids," J. Chem. Phys. **125**, 014505, (2006).

[7]P. Mausbach and H.-O. May, "Direct molecular simulation of the Grüneisen parameter and density scaling exponent in fluid systems," Fluid. Phase Equil. **366**, 108-116, (2014).

[8]J. C. Dyre, "Hidden Scale Invariance in Condensed Matter," J. Phys. Chem. B **118**, 10007-10024, (2014).

[9]O. L. Anderson, "The Grüneisen Ratio for the Last 30 Years," Geophys. J. Int. **143**, 279-294, (2000).

[10]D. J. Stevenson, "Application of Liquid State Physics to Earth's Core," Phys. Earth Planet. Interiors **2**, 42-62, (1980).

[11]E. W. Lemmon, U. Overhoff, M. O. McLinden and W. Wagner, to be submitted to J. Phys. Chem. Ref. Data, (2016).

[12]M. Thol, G. Rutkai, A. Köster, R. Lustig, R. Span, and J. Vrabec, "Equation of State for the Lennard-Jones Fluid," J. Phys. Chem. Ref. Data, in press, (2016).

[13]L. Knopoff and J. N. Shapiro, "Pseudo-Grüneisen parameter for Liquids," Phys. Rev. B **1**, 3893-3895, (1970).

[14]S. K. Kor, U. S. Tandon, and B. K. Singh, "Pseudo-Grüneisen parameter for liquid argon," Phys. Lett. **38A**, 187-188, (1972).

[15]R. Boehler and G. C. Kennedy, "Pressure Dependence of the thermodynamical Grüneisen parameter of fluids," J. Appl. Phys. **48**, 4183-4186, (1977).

[16]R. Boehler, "Melting temperature, adiabats, and Grüneisen parameter of lithium, sodium and potassium versus pressure," Phys. Rev. B **27**, 6754-6762, (1983).

[17]B. K. Sharma, "Volume dependence of thermodynamical Grüneisen parameter of fluorocarbon fluids," Phys. Lett. **99A**, 227-229, (1983).

[18]J. Amoros, J. R. Solana, and E. Villar, "Temperature, pressure and volume dependence of the Grüneisen parameter of dense gaseous and liquid argon," Mater. Chem. Phys. **20**, 255-260, (1988).

[19]R. Lustig, "Direct molecular NVT simulation of the isobaric heat capacity, speed of sound and Joule-Thomson coefficient," Mol. Sim. **37**, 457-465, (2011).

[20]R. Lustig, "Statistical analogues for fundamental equation of state derivatives," Mol. Phys. **110**, 3041-3052, (2012).

[21]S. Deublein, B. Eckl, J. Stoll, S. V. Lishchuk, G. Guevara-Carrion, C. W. Glass, T. Merker, M. Bernreuther, H. Hasse, and J. Vrabec, "*ms*2: A molecular simulation tool for thermodynamic properties," Comp. Phys. Commun. **182**, 2350-2367, (2011).

[22]C. W. Glass, S. Reiser, G. Rutkai, S. Deublein, A. Köster, G. Guevara-Carrion, A. Wafai, M. Horsch, M. Bernreuther, T. Windmann, H. Hasse, and J. Vrabec, "*ms*2: A molecular simulation tool for thermodynamic properties, new version release," Comp. Phys. Commun. **185**, 3302-3306, (2014).

[23]R. Span, *Multiparameter Equations of State: An Accurate Source of Thermodynamic Property Data*, Springer Verlag, Berlin, (2000).

[24]J. A. Barker and R. O Watts, "Monte Carlo studies of the dielectric properties of water-like models," Mol. Phys. **26**, 789-792, (1973).

[25]NIST Reference Fluid Thermodynamic and Transport Properties Database. http://www.nist.gov/srd/nist23.cfm.

[26]See supplemental material at [URL AIP] for the discussion of the temperature-dependent Grüneisen parameter for 15 additional substances.

[27]E. W. Lemmon and R. Span, "Short Fundamental Equations of State for 20 Industrial Fluids," J. Chem. Eng. Data **51**, 785-850, (2006).

[28]R. Tillner-Roth, F. Harms-Watzenberg and H. D. Baehr, "Eine neue Fundamentalgleichung für Ammoniak," DKV-Tagungsbericht **20**, 167-181, (1993).

[29]C. Tegeler, R. Span and W. Wagner, "A New Equation of State for Argon Covering the Fluid Region for Temperatures from the Melting Line to 700 K at Pressures up to 1000 MPa," J. Phys. Chem. Ref. Data **28**, 779-850, (1999).

[30]M. Thol, E. W. Lemmon and R. Span, "Equation of state for benzene for temperatures from the melting line up to 725 K with pressures up to 500 MPa," High Temperature - High Pressures **41**, 81-97, (2012).

[31]R. Span and W. Wagner, "A New Equation of State for Carbon Dioxide Covering the Fluid Region from the Triple-Point Temperature to 1100 K at Pressures up to 800 MPa," J. Phys. Chem. Ref. Data **25**, 1509-1596, (1996).

[32]M. Thol, I. Alexandrov, R. Span and E. W. Lemmon, to be submitted to J. Chem. Eng. Data, (2016).

[33]Y. Zhou, J. Lin, S. G. Penoncello and E. W. Lemmon, "An Equation of State for the Thermodynamic Properties of Cyclohexane," J. Phys. Chem. Ref. Data **43**, 043105, (2014).

[34]J. Wu, Y. Zhou and E. W. Lemmon, "An equation of state for the thermodynamic properties of dimethyl ether," J. Phys. Chem. Ref. Data **40**, 023104, (2011).

[35]D. Bücker and W. Wagner, "A Reference Equation of State for the Thermodynamic Properties of Ethane for Temperatures from the Melting Line to 675 K and Pressures up to 900 MPa," J. Phys. Chem. Ref. Data **35**, 205-266, (2006).

[36]J. A. Schroeder, "A New Fundamental Equation for Ethanol," Master's Thesis, University of Idaho, (2011).

[37]J. Smukala, R. Span and W. Wagner, "A New Equation of State for Ethylene Covering the Fluid Region for Temperatures from the Melting Line to 450 K at Pressures up to 300 MPa," J. Phys. Chem. Ref. Data **29**, 1053-1122, (2000).

[38]M. Thol, G. Rutkai, A. Köster, M. Kortmann, R. Span and J. Vrabec, "Fundamental equation of state for ethylene oxide based on a hybrid dataset," Chem. Eng. Sci. **121**, 87-99 (2015); Corrigendum, Chem. Eng. Sci. **134**, 887-890, (2015).

[39]K. M. de Reuck, "International Thermodynamic Tables of the Fluid State-11 Fluorine," International Union of Pure and Applied Chemistry, Pergamon Press, Oxford, (1990).

[40]M. Thol, F. H. Dubberke, G. Rutkai, T. Windmann, A. Köster, R. Span and J. Vrabec, "Fundamental equation of state correlation for hexamethyldisiloxane based on experimental and molecular simulation data," Fluid Phase Equilib. **418**, 133-151, (2016).

[41]M. Thol, L. Piazza and R. Span, "A New Functional Form for Equations of State for Some Polar and Weakly Associating Fluids," Int. J. Thermophys. **35**, 783-811, (2014).

[42]K. M. de Reuck and R. J. B. Craven, "Methanol, International Thermodynamic Tables of the Fluid State - 12," IUPAC, Blackwell Scientific Publications, London, (1993).

[43]R. Span, E. W. Lemmon, R. T. Jacobsen, W. Wagner and A. Yokozeki, "A Reference Equation of State for the Thermodynamic Properties of Nitrogen for Temperatures from 63.151 to 1000 K and Pressures to 2200 MPa," J. Phys. Chem. Ref. Data **29**, 1361-1433, (2000).

[44]M. Thol, G. Rutkai, A. Köster, F. H. Dubberke, T. Windmann, R. Span, and J. Vrabec, "Fundamental equation of state correlation for octamethylcyclotetrasiloxane based on experimental and molecular simulation data," to be submitted to J. Chem. Eng. Data, (2016).

[45]R. Schmidt and W. Wagner, "A New Form of the Equation of State for Pure Substances and its Application to Oxygen," Fluid Phase Equilib. **19**, 175-200, (1985).

[46]G. Rutkai and J. Vrabec, "Empirical fundamental equation of state for phosgene based on molecular simulation data," J. Chem. Eng. Data **60**, 2895-2905, (2015).

[47]A. Polt, B. Platzer and G. Maurer, "Parameter der thermischen Zustandsgleichung von Bender fuer 14 mehratomige reine Stoffe," Chem. Tech. (Leipzig) **44**, 216-224, (1992).

[48]W. Wagner and A. Pruss, "The IAPWS Formulation 1995 for the Thermodynamic Properties of Ordinary Water Substance for General and Scientific Use," J. Phys. Chem. Ref. Data

31, 387-535, (2002).

[49]E. W. Lemmon and R. Span, "Thermodynamic Properties of R-227ea, R-365mfc, R-115, and R-13—1," J. Chem. Eng. Data **60**, 3745-3758, (2015).

[50]T. Windmann, M. Linnemann, and J. Vrabec, "Fluid phase behavior of Nitrogen+ Acetone and Oxygen+ Acetone by molecular simulation, experiment and the Peng-Robinson equation of state," J. Chem. Eng. Data **59**, 28-38 (2013).

[51]B. Eckl, J. Vrabec and H. Hasse, "An optimised molecular model for ammonia," Mol. Phys. **106**, 1039-1046, (2008).

[52]J. Vrabec, J. Stoll and H. Hasse, "A set of molecular models for symmetric quadrupolar fluids," J. Phys. Chem. B **105**, 12126-12133, (2001).

[53]Y.-L. Huang, M. Heilig, H. Hasse and J. Vrabec, "Vapor-liquid equilibria of hydrogen chloride, phosgene, benzene, chlorobenzene, ortho-dichlorobenzene, and toluene by molecular simulation," AIChE J. **57**, 1043-1060, (2011).

[54]T. Merker, C. Engin, J. Vrabec and H. Hasse, "Molecular model for carbon dioxide optimized to vapor-liquid equilibria," J. Chem. Phys. **132**, 234512, (2010).

[55]J. Stoll, J. Vrabec and H. Hasse, "A set of molecular models for carbon monoxide and halogenated hydrocarbons," J. Chem. Phys. **119**, 11396-11407, (2003).

[56]T. Merker, J. Vrabec and H. Hasse, "Molecular simulation study on the solubility of carbon dioxide in mixtures of cyclohexane+ cyclohexanone" Fluid Phase Equilib. **315**, 77-83, (2012).

[57]B. Eckl, J. Vrabec and H. Hasse, "Set of molecular models based on quantum mechanical ab initio calculations and thermodynamic data," J. Phys. Chem. B **112**, 12710-12721, (2008).

[58]T. Schnabel, J. Vrabec and H. Hasse, "Henrys law constants of methane, nitrogen, oxygen and carbon dioxide in ethanol from 273 to 498 K: Prediction from molecular simulation," Fluid Phase Equilib. **233**, 134-143, (2005).

[59]B. Eckl, J. Vrabec and H. Hasse, "On the Application of Force Fields for Predicting a Wide Variety of Properties: Ethylene Oxide as an Example," Fluid Phase Equilib. **274**, 16-26, (2008).

[60]T. Kristóf and J. Liszi, "Effective intermolecular potential for fluid hydrogen sulfide," J. Phys. Chem. B **101**, 5480-5483, (1997).

[61]T. Schnabel, A. Srivastava, J. Vrabec and H. Hasse, "Hydrogen bonding of methanol in supercritical CO2: comparison between 1H NMR spectroscopic data and molecular simulation results," J. Phys. Chem. B **111**, 9871-9878, (2007).

[62]J. L. Abascal and C. Vega, "A general purpose model for the condensed phases of water: TIP4P/2005," J. Chem. Phys. **123**, 234505, (2005).

[63]B. Eckl, Y.-L. Huang, J. Vrabec and H. Hasse, "Vapor pressure of R227ea+ethanol at 343.13 K by molecular simulation," Fluid Phase Equilib. **260**, 177-182, (2007).

[64]G. Rutkai, M. Thol, R. Lustig, R. Span, and J. Vrabec, "Communication: Fundamental equation of state correlation with hybrid data sets," J. Chem. Phys. **139**, 041102, (2013).

[65]R. T. Jacobsen and R. B. Stewart, "Thermodynamic properties of nitrogen including liquid and vapor phases from 63K to 2000K with pressures to 10,000 bar," J. Phys. Chem. Ref. Data **2**, 757-922, (1973).

[66]H.-O. May and P. Mausbach, "Riemannian geometry study of vapor-liquid phase equilibria and supercritical behavior of the Lennard-Jones fluid," Phys. Rev. E **85**, 031201, (2012), Phys. Rev. E **86**, 059905(E), (2012).

[67]V. Holten, M. A. Anisimov, and J. V. Sengers, Technical Report prepared for the International Association for the Properties of Water and Steam (2012), http://www.iapws.org/minutes/2012/Holten2012-report.pdf.

[68]F. Mallamace, C. Corsaro, and H. E. Stanley, "A singular thermodynamically consistent temperature at the origin of the anomalous behavior of liquid water," Sci. Rep. **2**, 993, (2012).

[69]G. Ruppeiner, P. Mausbach, and H.-O. May, "Thermodynamic R-diagrams reveal solid-like fluid states," Phys. Lett. A, **379**, 646-649, (2015).

[70]H.-O. May, P. Mausbach, and G. Ruppeiner, "Thermodynamic geometry of supercooled water," Phys. Rev. E **91**, 032141, (2015).

[71]P. Colonna, A. Guardone, and N.R. Nannan, "Siloxanes: A new class of candidate Bethe-Zel'dovich-Thompson fluids," Phys. Fluids **19**, 086102, (2007).

[72]P. Colonna, N.R. Nannan, A. Guardone, and T.P. van der Stelt, "On the computation of the fundamental derivative of gas dynamics using equations of state," Fluid Phase Equilib. **286**, 4354, (2009).

[73]A. Köster, T. Spura, G. Rutkai, J. Kessler, H. Wiebeler, J. Vrabec, and T.D. Kühne, "Assessing the accuracy of improved force-matched water models derived from ab-initio molecular dynamics simulations," J. Comput. Chem., doi: 10.1002/jcc.24398, (2016).

Supporting Information to: Comparative study of the Grüneisen parameter for 28 pure fluids

Peter Mausbach,[1] Andreas Köster,[2] Gábor Rutkai,[2] Monika Thol,[3] and Jadran Vrabec[2, a)]

[1)] *Cologne University of Applied Sciences, 50678 Köln/Germany*

[2)] *Thermodynamics and energy technology, Universität Paderborn, 33098 Paderborn/Germany*

[3)] *Thermodynamics, Ruhr-Universität Bochum, 44801 Bochum/Germany*

(Dated: 1 July 2016)

This supplementary material contains additional figures of the temperature-dependent Grüneisen parameter for 15 substances.

[a)] Corresponding author. E-mail address: jadran.vrabec@upb.de

I. LINEAR, QUADRUPOLAR MOLECULES

Figs. S1 to S4 show the temperature-dependent Grüneisen parameter of fluorine, oxygen, propyne and propylene, respectively. For fluorine, a good agreement between simulation and EOS data exists only for densities up to $\rho \approx 10$ mol/l. For densities $\rho > 10$ mol/l, the isochores obtained from the EOS increase with increasing temperature. The rates of change of γ_{G} increase as the density is increased. This behavior is in contrast to the expected temperature-dependence. The EOS results in Fig. S1 reflect the incorrect thermodynamic behavior of γ_{G} of fluorine discussed in Fig. 16.a in the main paper. The simulated Grüneisen parameter of oxygen (Fig. S2) follows the general (ρ, T) trend. A comparison with values calculated from the corresponding EOS shows large deviations at high densities. Here, the isochores extrapolated from the EOS develop a minimum, which is inconsistent with the general behavior of γ_{G}. For propyne (Fig. S3), a reasonable agreement between simulation data and EOS values exists only for the lowest densities. Significant deviations at high densities can be attributed to the incorrect behavior of the EOS as discussed in Fig. 16.b in the main part of the paper. The (ρ, T) behavior of γ_{G} for propylene is shown in Fig. S4. A very good agreement between simulated and EOS data can be observed even at high densities.

II. TRIANGULAR, DIPOLAR MOLECULES

Figs. S5 and S6 show the temperature dependence of the Grüneisen parameter γ_{G} of dimethylether and sulfur dioxide. For dimethylether, the agreement

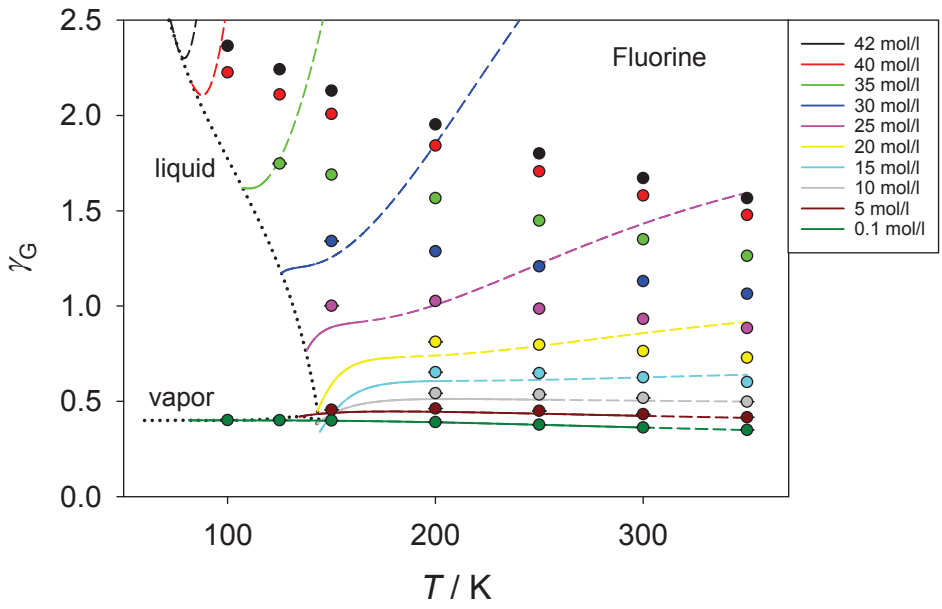

FIG. S1. Grüneisen parameter γ_G of fluorine as a function of temperature along different isochores ranging from $\rho = 0.1$ to 42 mol/l.

between simulation and EOS results is good for densities up to $\rho \approx 10$ mol/l. Increasing deviations occur at high densities, where the EOS was extrapolated. For sulfur dioxide, reasonably good agreement is found between simulation and EOS data, except for the region close to the liquid saturation line. The simulated Grüneisen parameter reveals the expected temperature-dependence, whereas the γ_G isochores obtained from the EOS develop a maximum near the saturation line even at high densities.

III. HYDROGEN BONDING MOLECULES

Figs. S7 to S10 show the temperature-dependent Grüneisen parameter of ammonia, ethanol, methanol and hydrogen sulfide, respectively. In the dense liquid phase of ammonia (Fig. S7) remarkable deviations between simulation results

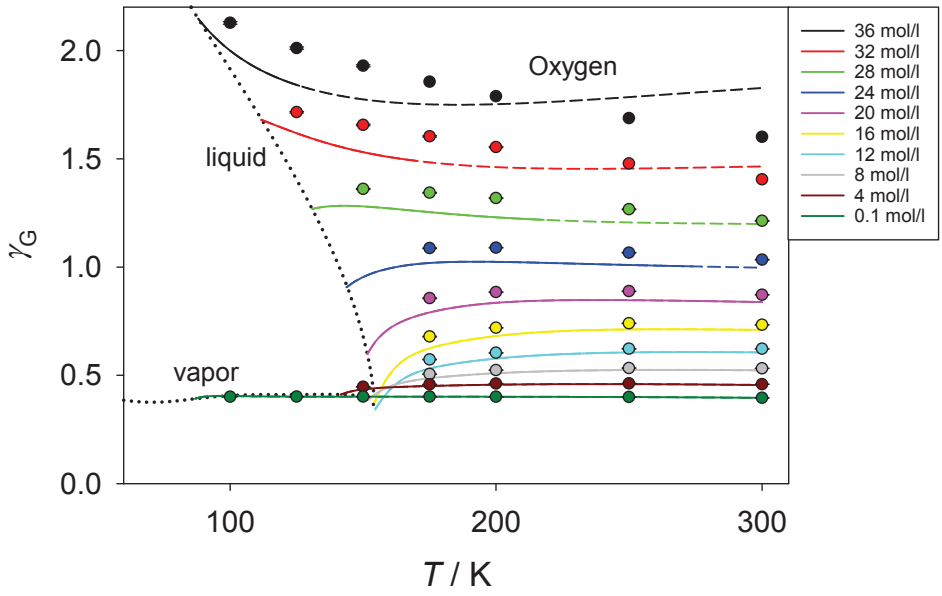

FIG. S2. Grüneisen parameter γ_G of oxygen as a function of temperature along different isochores ranging from $\rho = 0.1$ to 36 mol/l.

and EOS values are present. For ethanol and methanol, large deviations occur between simulation and EOS data particularly at high densities. The simulated isochores show the expected behavior for both substances. Two weak extrema appear along the EOS isochore of ethanol at $\rho = 18$ mol/l (Fig. S8). For methanol (Fig. S9), the large deviations at high densities increase with increasing temperature. For hydrogen sulfide, the temperature dependence of γ_G from simulation and EOS agrees reasonably well if the density is not too high, cf. Fig. S10.

IV. CYCLIC MOLECULES

Figs. S11, S12 and S13 show the temperature dependence of the Grüneisen parameter γ_G of benzene, chlorobenzene and toluene. All three substances exhibit larger deviations between simulation and EOS values especially at higher

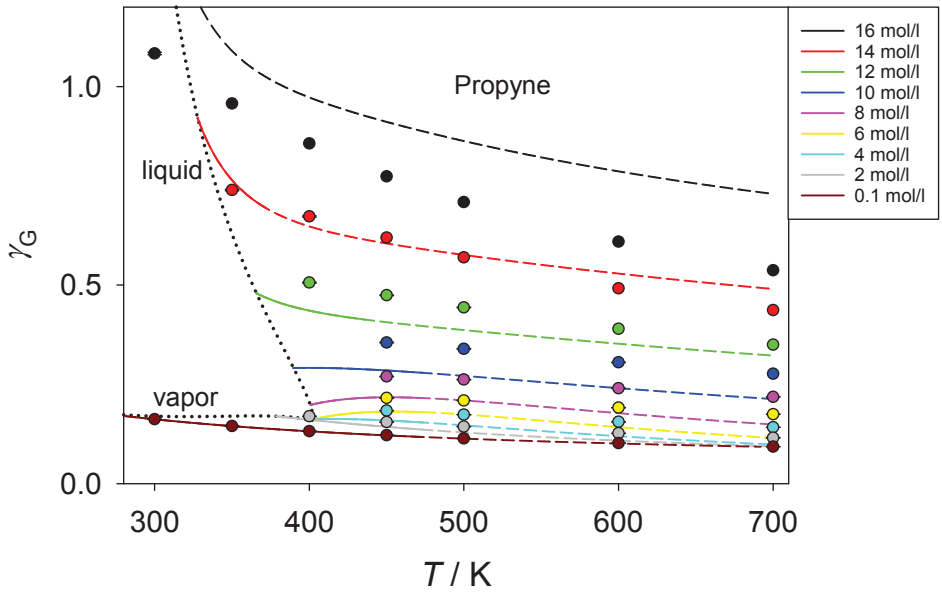

FIG. S3. Grüneisen parameter γ_G for propyne as a function of temperature along different isochores ranging from $\rho = 0.1$ to 16 mol/l.

densities. However, the general (ρ, T) trend was confirmed by simulation and the associated EOS for all three fluids.

V. SILOXANES

Fig. S14 shows the temperature-dependent behavior of the Grüneisen parameter of octamethylcyclotetrasiloxane. Similar to hexamethyldisiloxane, an extended fitting strategy was applied to develop an EOS with a high accuracy. A good agreement between simulated and EOS data can be observed.

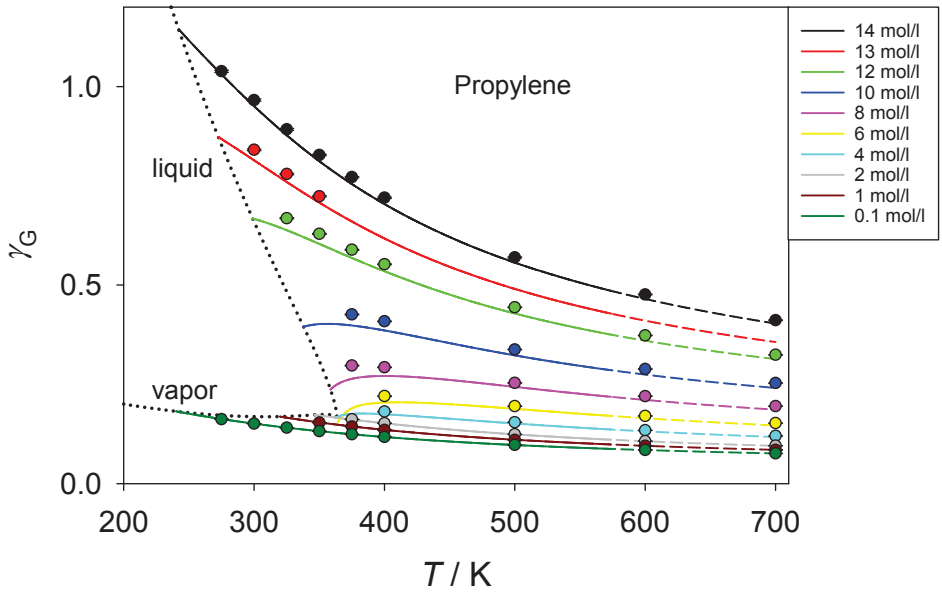

FIG. S4. Grüneisen parameter γ_G of propylene as a function of temperature along different isochores ranging from $\rho = 0.1$ to 14 mol/l.

VI. OTHER FLUIDS

In Fig. S15 the phase behavior of the Grüneisen parameter is presented for 1,1,1,2,3,3,3-heptafluoropropane, an HFC fluid designed to replace R114 that is used for refrigeration and heat pump applications. The agreement between the corresponding EOS and present simulation results is reasonably good except along the $\rho = 10$ mol/l isochore at high temperatures.

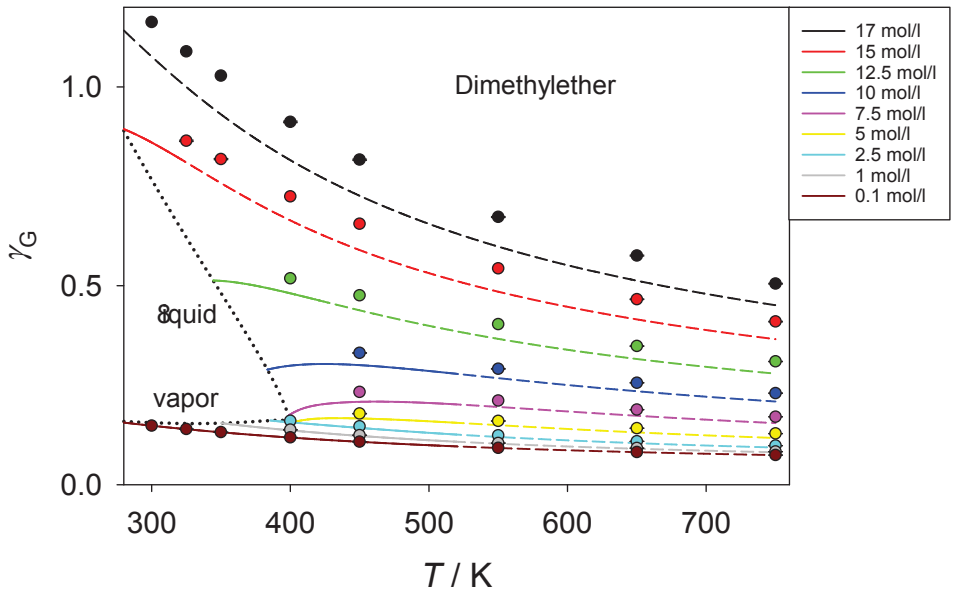

FIG. S5. Grüneisen parameter γ_G of dimethylether as a function of temperature along different isochores ranging from $\rho = 0.1$ to 17 mol/l.

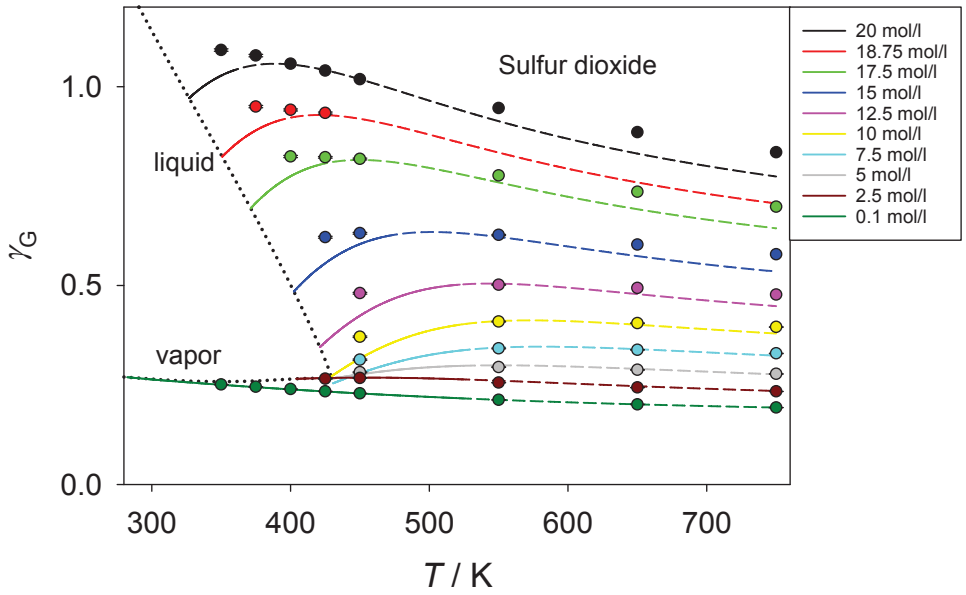

FIG. S6. Grüneisen parameter γ_G of sulfur dioxide as a function of temperature along different isochores ranging from $\rho = 0.1$ to 20 mol/l.

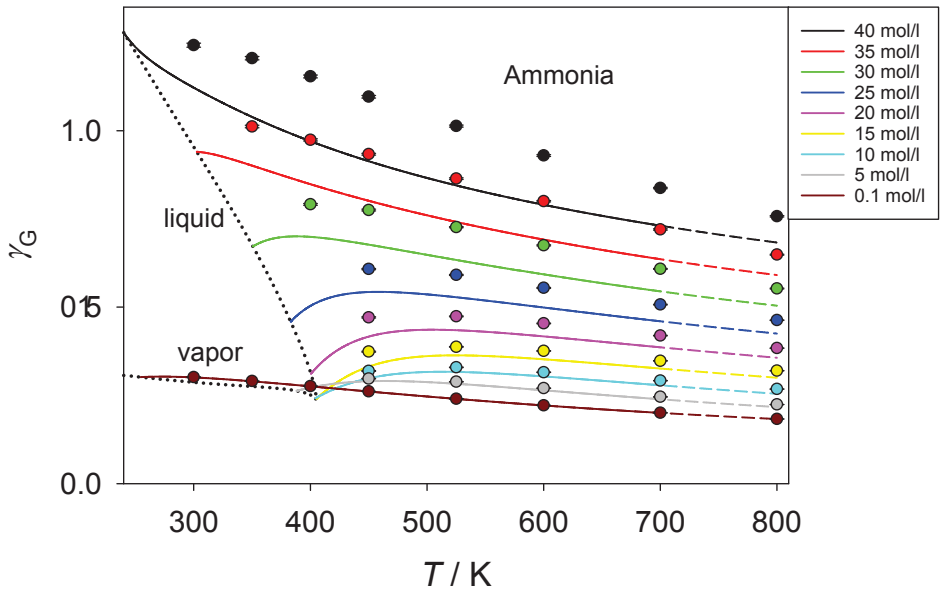

FIG. S7. Grüneisen parameter γ_G of ammonia as a function of temperature along different isochores ranging from $\rho = 0.1$ to 40 mol/l.

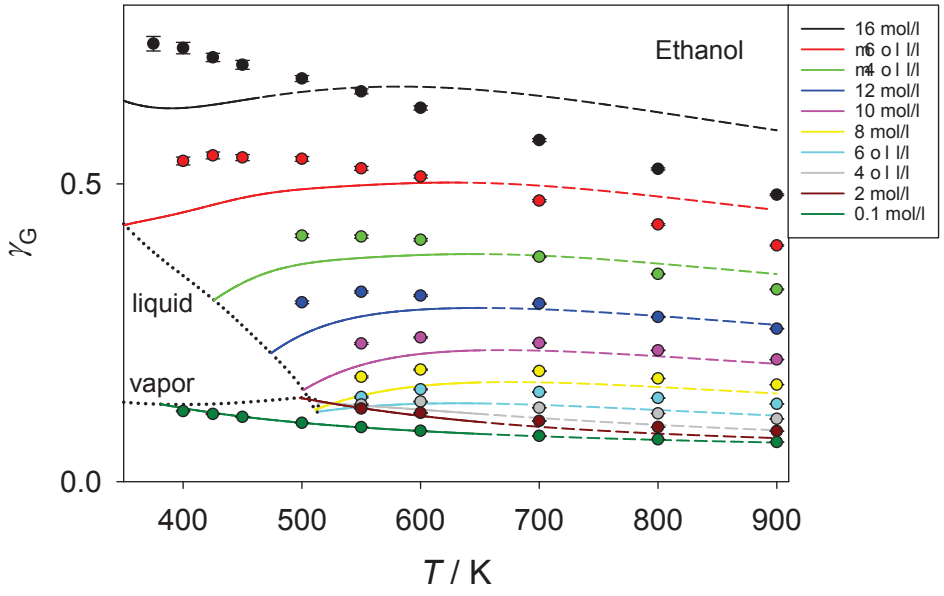

FIG. S8. Grüneisen parameter γ_G of ethanol as a function of temperature along different isochores ranging from $\rho = 0.1$ to 18 mol/l.

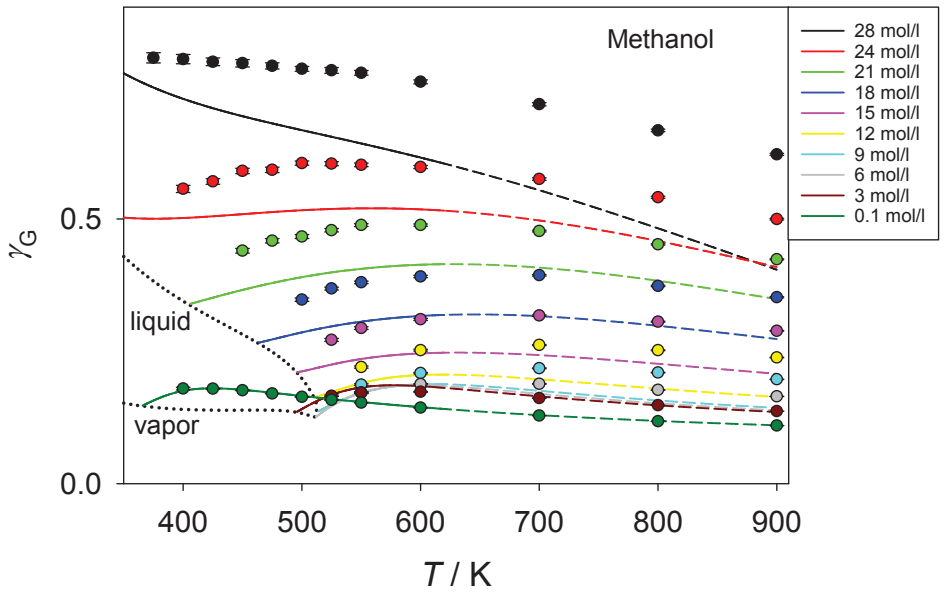

FIG. S9. Grüneisen parameter γ_G of methanol as a function of temperature along different isochores ranging from $\rho = 0.1$ to 28 mol/l.

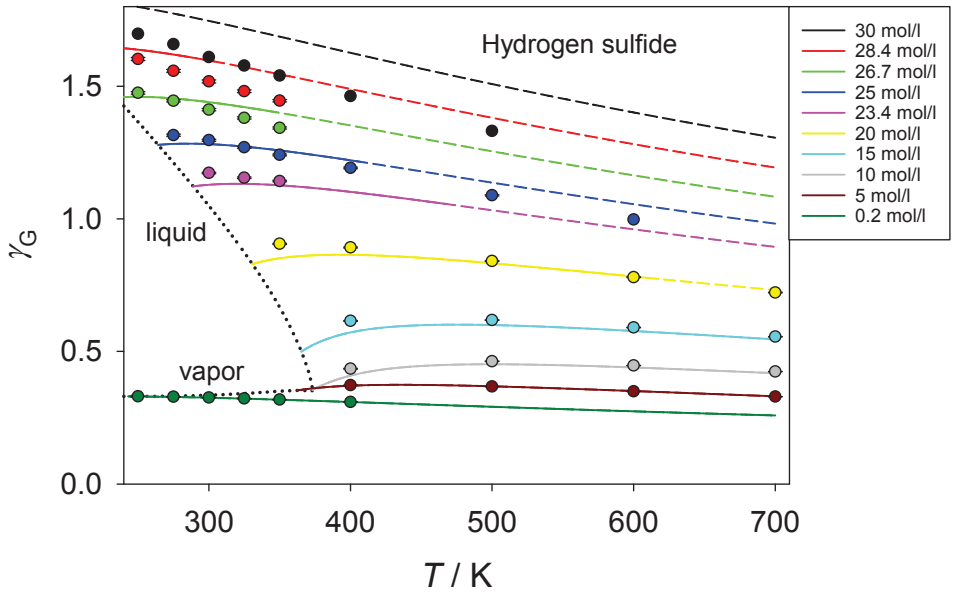

FIG. S10. Grüneisen parameter γ_G of hydrogen sulfide as a function of temperature along different isochores ranging from $\rho = 0.2$ to 30 mol/l.

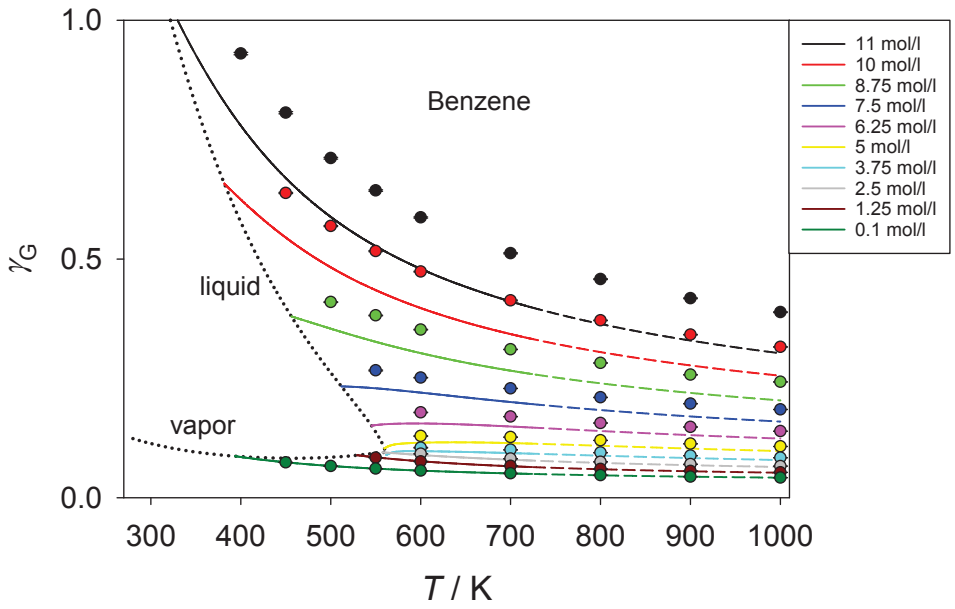

FIG. S11. Grüneisen parameter γ_G of benzene as a function of temperature along different isochores ranging from $\rho = 0.1$ to 11 mol/l.

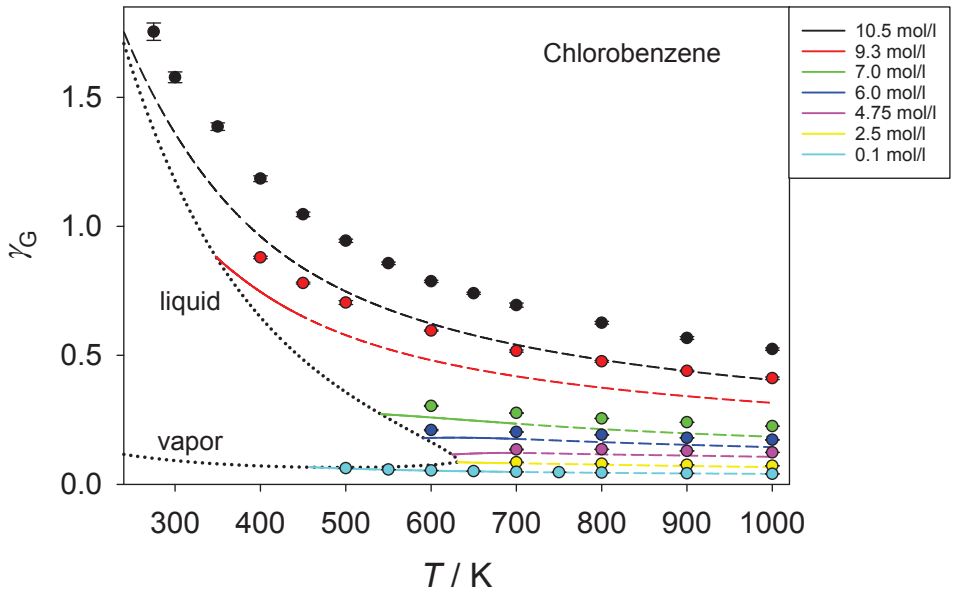

FIG. S12. Grüneisen parameter γ_G of chlorobenzene as a function of temperature along different isochores ranging from $\rho = 0.1$ to 10.5 mol/l.

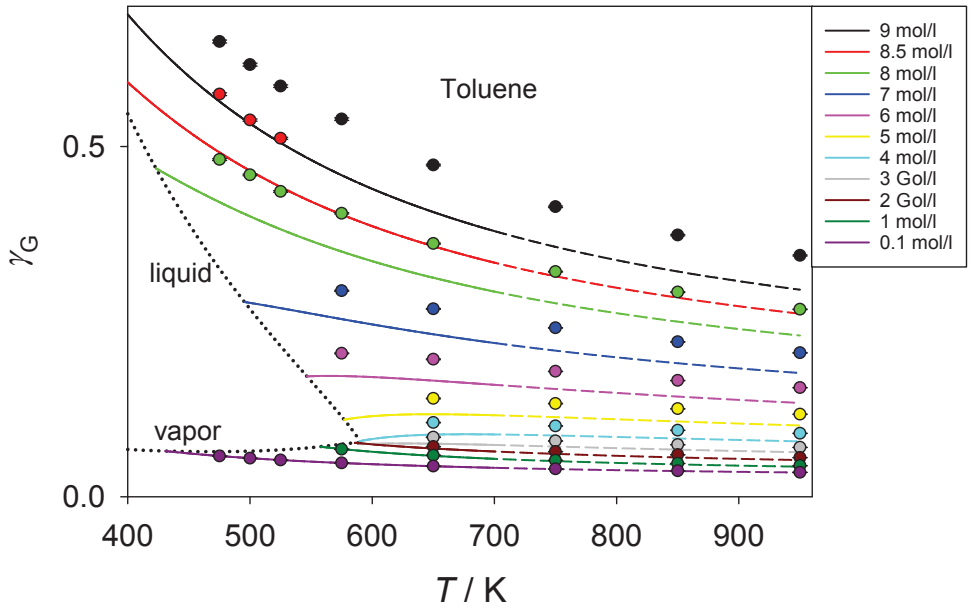

FIG. S13. Grüneisen parameter γ_G of toluene as a function of temperature along different isochores ranging from $\rho = 0.1$ to 9 mol/l.

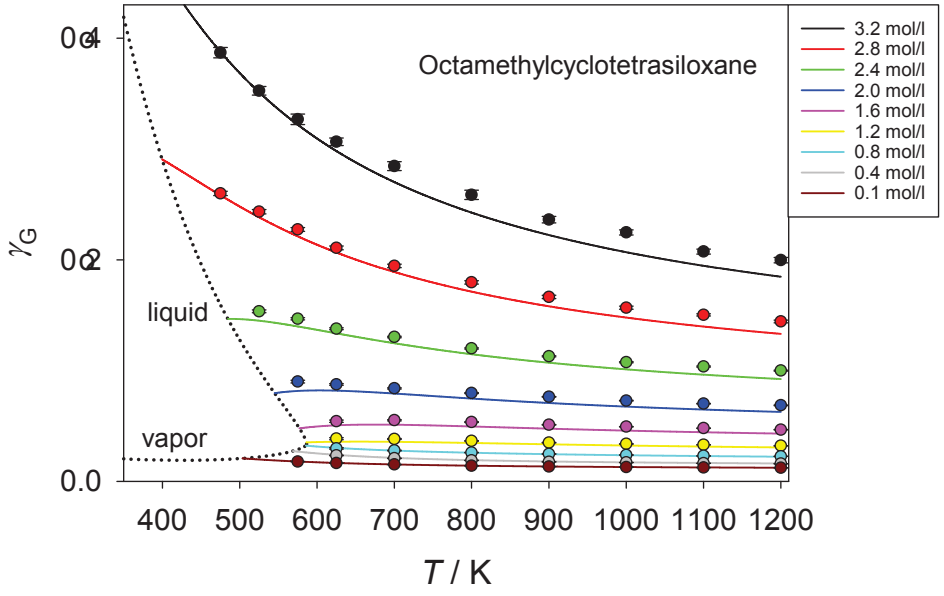

FIG. S14. Grüneisen parameter γ_G of octamethylcyclotetrasiloxane as a function of temperature along different isochores ranging from $\rho = 0.1$ to 3.2 mol/l.

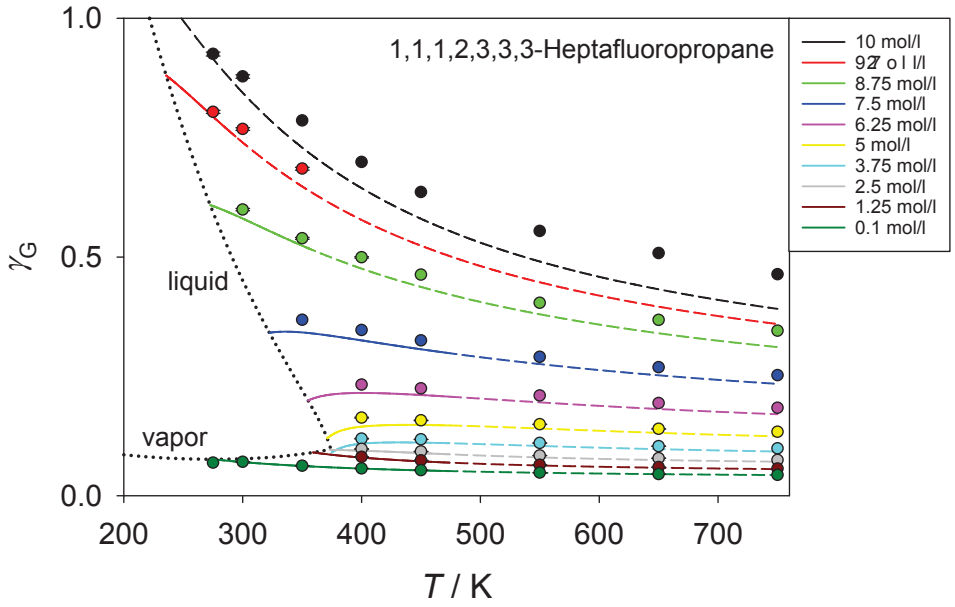

FIG. S15. Grüneisen parameter γ_G of 1,1,1,2,3,3,3-heptafluoropropane as a function of temperature along different isochores ranging from $\rho = 0.1$ to 10 mol/l.